REMOVAL OF PARACETAMOL ON BIOMASS-DERIVED ACTIVATED CARBON: MODELING THE FIXED BED BREAKTHROUGH CURVES USING BATCH ADSORPTION EXPERIMENTS

F.J. García-Mateos, R. Ruiz-Rosas, M.D. Marqués, L.M. Cotoruelo, J. Rodríguez-Mirasol*, T. Cordero

Universidad de Málaga, Andalucía Tech, Departamento de Ingeniería Química, Escuela Técnica Superior de Ingeniería Industrial, Campus de Teatinos s/n, 29071 Málaga, Spain.

To be submitted to: CHEMICAL ENGINEERING JOURNAL

*Corresponding author. Tel.: +34 951 952 385. E-mail: mirasol@uma.es (José Rodríguez Mirasol)

Nomenclature (units used)

a	empirical parameter (s^{-1})
A_{BET}	specific surface area by Brunauer, Emett, Teller method ($m^2\ g^{-1}$)
A_{DR}	Dubinin Radushkevich surface area ($m^2\ g^{-1}$)
A_t	external area ($m^2\ g^{-1}$)
B	time constant (s^{-1})
b	empirical parameter ($m^2\ s^{-1}$)
c	empirical parameter (s)
C	outlet concentration ($mg\ L^{-1}$)
C_0	initial concentration ($mg\ L^{-1}$)
C_b	paracetamol bed concentration ($mol\ m^{-3}$)
C_e	equilibrium concentration ($mg\ L^{-1}$)
C_i	inlet concentration ($mg\ L^{-1}$)
C_p	concentration in the particle external surface ($mol\ m^{-3}$)
C_t	concentration at time t ($mg\ L^{-1}$)
d	empirical parameter (s)
D_e	effective internal diffusion coefficient ($m^2\ s^{-1}$)
D_l	molecular diffusivity of the solute in water ($m^2\ s^{-1}$)
D_s	surface diffusion coefficient ($m^2\ s^{-1}$)

41 D_z axial dispersion coefficient ($m^2\ s^{-1}$)

42 k_f external film mass-transfer coefficient ($m\ s^{-1}$)

43 k_i intraparticle mass transfer (s^{-1})

44 K_L equilibrium constant of Langmuir equation ($L\ mg^{-1}$)

45 K_{L0} pre-exponential factor in Langmuir equation ($L\ mg^{-1}$)

46 L_b bed length (cm)

47 N number of transfer units

48 N_S diffusion molar flux ($mol\ m^{-2} \cdot s^{-1}$)

49 Q flow rate ($mL\ min^{-1}$)

50 $\bar{q}$ mean concentration of solute adsorbed in the adsorbent particle

51 q_{cal} calculated adsorption capacity from models at $C/C_i = 0.95$ ($mg\ g^{-1}$)

52 $q|_{Cp}$ adsorbed concentration at the solid external surface

53 q_e adsorption capacity at equilibrium ($mg\ g^{-1}$)

54 q_{exp} experimental adsorption capacity at $C/C_i \approx 0.95$ ($mg\ g^{-1}$)

55 q_i adsorption capacity at C_i concentration ($mg\ g^{-1}$)

56 q_L maximum adsorption capacity at equilibrium of Langmuir equation ($mg\ g^{-1}$)

57 q_m empirical parameter ($mg\ g^{-1}$)

58 q_r adsorbed concentration at r radial position in the particle ($mol\ m^{-3}$)

59 q_t adsorption capacity at time t ($mg\ g^{-1}$)

60	R	gases constant (8.31 J $mol^{-1} \cdot K^{-1}$)
61	R_b	bed radius (cm)
62	R_p	particle size (mm)
63	R_S	separation factor
64	r^2	determination coefficient
65	T	throughput parameter
66	t	time (min)
67	t_s	stoichiometric time (min)
68	u	superficial liquid velocity (m s^{-1})
69	V_b	molar volume of solute at the normal boiling point (cm^3 mol^{-1})
70	V_{DR}	Dubinin Radushkevich narrow micropore volume (cm^2 g^{-1})
71	V_{mes}	mesopore volume from the N_2 isotherm (cm^3 g^{-1})
72	V_p	total pore volume from the N_2 isotherm (cm^3 g^{-1})
73	V_t	micropore volume from the N_2 isotherm (cm^3 g^{-1})
74	v_z	axial velocity (m s^{-1})
75	w	adsorbent dose (g L^{-1})
76	W	mass of activated carbon (mg)
77	z	axial position in bed
78		

Greek characters

ε_b	bed porosity
ε_p	particle porosity
μ_l	fluid dynamic viscosity (cP)
η	yield
ρ_b	bed density (kg m^{-3})
ρ_l	fluid density (kg m^{-3})
ρ_p	particle density (kg m^{-3})

Abstract

The remediation of paracetamol (PA), an emerging contaminant frequently found in wastewater treatment plants, has been studied in the low concentration range (0.3-10 mg L^{-1}) using as adsorbent a biomass-derived activated carbon. PA uptake of up to 100 mg g^{-1} over the activated carbon has been obtained, with the adsorption isotherms being fairly explained by the Langmuir model. The application of Reichemberg and the Vermeulen equations to the batch kinetics experiments allowed estimating homogeneous and heterogeneous diffusion coefficients, reflecting the dependence of diffusion with the surface coverage of PA. A series of rapid small-scale column tests were carried out to determine the breakthrough curves under different operational conditions (temperature, PA concentration, flow rate, bed length). The suitability of the proposed adsorbent for the remediation of PA in fixed-bed adsorption was proven by the high PA adsorption capacity along with the fast adsorption and the reduced height of the mass transfer zone of the columns. We have demonstrated that, thanks to the use of the heterogeneous diffusion coefficient, the proposed mathematical approach for the numerical solution to the mass balance of the column provides a reliable description of the breakthrough profiles and the design parameters, being much more accurate than models based in the classical linear driving force.

Keywords: Activated carbon, Adsorption, Paracetamol, Pharmaceuticals, Column adsorption, Modeling breakthrough curves

Highlights

- Activated carbon with well-developed porosity has been prepared from a biomass waste
- It shows high removal efficiency of paracetamol in low concentrations (0.3-10 mg L^{-1})
- Uptake of ca. 100 mg g^{-1} and narrow mass transfer zone is observed in fixed-bed adsorption
- Heterogeneous diffusivity coefficient successfully describes the adsorption kinetics
- Breakthrough curves are predicted using adsorption parameters of batch experiments

1. Introduction

Pharmaceutical compounds are labeled as emerging environment pollutants because, as in the case of many other every-day use and personal care products, they are found in increasing amounts in urban and industrial wastewaters, and even in surface waters [1], [2] and [3]. Since these compounds have biological activity, there exist scientific and social concerns to control the impact of these micropollutants on the environmental systems. Although many of these compounds have been proved to be rather stable and can generate bioaccumulation and biomagnification processes, they do not need to persist in the environment to cause negative effects, since their elimination or transformation is compensated by daily continuous introduction, derived of discharges and elution from pharmaceutical production plants, hospitals, homes or landfills. It is possible to find a great number of studies that analyze their concentration in streams, rivers, ground, surface or drinking water. They report how efficiently the municipal wastewater plants are in their removal, providing consistent proofs of the low removal efficiency for broad groups of pharmaceutical compounds making necessary the implementation of additional wastewater treatments for their remediation [1], [4], [5] and [6]. More specifically, there are several works detailing the occurrence of pharmaceutical compounds in surface waters in concentrations that ranges from 10^{-9} to 10^{-6} g L^{-1}. For instance, some studies realized in Spanish rivers, [7] and [8], showed the presence of a great variety of soluble pharmaceutical compounds.

The adsorption in fixed beds columns with activated carbon is one of the most efficient advanced methods to remove organic micropollutants from aqueous effluents. Activated carbon is broadly utilized in water and gas treatment due to its unmatched adsorption capacity and its competitive cost [9] and [10]. The removal efficiency of activated carbon are strongly dependent on tailoring its chemical and physical structure to match

the required properties for the application. On the one hand, the surface chemistry of the carbon should be to the least compatible for the adsorption of the pollutant in terms of polarity, acidity and aromatic degree. If adequately tuned, these properties can be profited for enhancing the removal efficiency of activated carbons [11], [12] and [13]. On the other hand, it is necessary to use adsorbents with a well-developed and reachable surface area, and reduced mass transfer limitations for enhancing the bed service time. In this sense, the accessibility to the micropores, which are responsible for most of the adsorption capacity of an activated carbon, can be enhanced by the presence of mesopores [14] and [15]. Thus, the adsorption equilibrium and kinetics for each specific contaminant are related to the chemical surface and the porous structure of the activated carbon used as adsorbent.

For envisaging the viability of activated carbons, it is critical to develop models and experimental procedures that could be used for accurately describing the dynamics of the pollutant adsorption and desorption under a variety of operating conditions from lab scale measurements. In this light, there has been considerable effort for determining these relationships using rapid small-scale column tests (RSSCT) [16]. These tests enable the design of fixed-bed activated carbon adsorbers in lab-scale that fairly reproduces the behavior of full-scale adsorbers [17], [18] and [19]. Even so, most of the laboratories are equipped for the determination of the thermodynamic and kinetic adsorption parameters using batch experiments, and the development of analytical tools for obtaining information of adsorbent performance in batch studies that would be relevant and valuable for predicting the removal performance of the adsorbents in fixed-bed adsorption is still necessary. The work herein aimed at conciliating removal performance as determined by batch and column experiments of a model organic micropollutant by a specifically made biomass-derived activated carbon, so that easy

and readily applicable protocols in batch configuration can be used to identify the adsorption isotherms and diffusion properties of carbons for column operation.

The work herein details the removal of acetaminophen (paracetamol) at low concentrations (<10 mg L^{-1}) by adsorption on a biomass-based activated carbon in column operation. Paracetamol (PA) is an analgesic worldwide consumed and it is ubiquitously found in European surface waters [6] and [8], therefore being selected as a model emerging contaminant. Paracetamol adsorption in activated carbon have been widely studied during the last decade by Prof. Terzyk [20] and some other research groups [21], [22] and [23], although in concentrations much higher than those currently registered in wastewater treatment plants. As pointed out before, the aim of this work is also related to validate the use of batch adsorption experiments for determining the adsorption parameters that can later be used to accurately describe the behavior of a small-scale column test. Thus, batch adsorption experiments were used to determine the paracetamol uptake, adsorption equilibrium as well as the kinetic parameters, which were later employed to calculate the breakthrough profiles for the lab-scale fixed-bed adsorption column. Two models, the first being a numerical solution to the paracetamol molar balance in the fixed-bed and carbon particle, where a heterogeneous diffusion coefficient in the pores related to the amount of adsorbed paracetamol is considered, and the second one being the commonly used constant pattern linear driving force model (CP-LDF), have been compared for the description of the breakthrough profiles. The modeled breakthrough profiles along with the service parameters of rapid small scale column tests were confronted with those experimentally obtained at laboratory, which allowed us to clarify how batch adsorption data should be worked out for achieving a successful description of the behavior of a given adsorbent in fixed-bed adsorption.

2. Materials and methods

2.1. Preparation and characterization of the activated carbon

Olive stones provided by Sociedad Cooperativa Andaluza Olivarera y Frutera San Isidro (Periana, Málaga) were used as the raw material. This abundant and economic residue constitutes an excellent and underutilized carbon precursor. It is not a porous material as supplied, and therefore it has not adsorption capacity by itself; an activation step is necessary to develop any specific surface area. Olive stones were previously grinded, washed with distilled water, and dried at 100 ºC before their use. The precursor was then impregnated with concentrated commercial H_3PO_4 (85 % wt, Sigma Aldrich), using a weight ratio of 3/1 (H_3PO_4/olive stone) at 60 ºC for 24 h. This activating agent is known to promote a high mesopore volume development in the resulting activated carbon [24] and [25], which is useful in liquid phase adsorption, as well as a rendering higher carbonization yield than other activation methods thanks to the catalytic aromatization that the biomass undergoes when contacted with phosphoric acid [26], which is beneficial for a better sustainability of the preparation process. The mixture was activated at 500 ºC under continuous N_2 (99.999%) flow (150 cm^3 min^{-1}) in a tubular furnace. The activation temperature was reached at a heating rate of 10 ºC min^{-1}, kept for 2 h and the activated sample was cooled inside the furnace until room temperature. The resulting activated carbon was washed with distilled water at 60 ºC to neutral pH and negative phosphate analysis in the eluate. A final heat treatment at 900 ºC under inert flow (N_2) was carried out, obtaining a thermally treated activated carbon (ACTT). The carbon was weighted to determine the yield of the preparation process (weight % of activated carbon related to weight of raw material, in dry basis, η=42.4%), grinded and sieved to a particle size between 0.3-0.1 mm.

219 The porous structure was characterized by N_2 adsorption-desorption at -196 ºC, and by
220 CO_2 adsorption at 0 ºC performed in ASAP 2020 equipment (Micromeritics). The
221 sample was previously outgassed at room temperature for at least 8 hours. From the N_2
222 isotherm, the apparent surface area (A_{BET}) was determined applying the BET equation
223 [27]. The micropore volume (V_t) and the external surface area (A_t) were calculated using
224 the t-method [28], [29] and [30] using a non-porous carbon black as standard. The
225 narrow mesopore volume (V_{mes}) was determined by the difference between the adsorbed
226 volume of N_2 at a relative pressure of 0.995 and the micropore volume (V_t). From the
227 CO_2 adsorption data, the narrow micropore volume (V_{DR}) and apparent surface area
228 (A_{DR}) were calculated using the Dubinin-Radushkevich equation [31]. The size, shape
229 and texture of the ACTT particles were analyzed by scanning electron microscopy
230 (SEM) in a JEOL JSM-840 instrument. Fig. 1 shows a micrograph of the ACTT. From
231 these and similar micrographs, carbon particle size (average range after sieving) was
232 estimated to be 185 ±5 µm. Therefore, a particle radius (R_p) of 92.5 µm and particle
233 density (ρ_p) of 1.294 g cm^{-3} measured by water displacement have been used as input
234 parameters for the mass balance equations.

235 **FIGURE 1 HERE**

236 Table 1 summarizes the surface properties of the activated carbon. High values for
237 surfaces area, a balanced meso to microporosity ratio (V_{mes}/V_t) and a high development
238 of wide microporosity ($V_t > V_{DR}$) are obtained, which constitute valuable features in a
239 diffusion-involved application as the liquid phase adsorption.

240 The surface chemistry of the sample was analyzed by X-ray photoelectron spectroscopy
241 (5700C model Physical Electronics) with Mg kα radiation (1253.6 eV). The maximum
242 of the C1s peak was set to 284.5 eV and used as reference for shifting the whole

spectrum. As can be seen in Table 1, the carbon used in this work presented surface phosphorus groups. The generation of surface phosphorus groups during H_3PO_4-activation of biomass have been long proven by our research group, while their striking influence in the surface acidity, kinetic activity and oxidation resistance of the resulting activated carbons have been reported in the past [32] and [33]. A detailed study of XPS P_{2p} region revealed that the thermal treatment produced a shift of the spectra to lower binding energies, which means that $COPO_3$ groups were thermal reduced by the surface of the activated carbon to form lesser oxidized species, such as CPO_3, C_2PO_2 and C_3PO, decreasing the surface acidity [34] and [35]. Since some authors [36] have linked the paracetamol adsorption capacity with the acidity and the carbonization temperature in phosphorus-containing activated carbons, it is expected that the heat treatment would produce a lower acidity and polarity of the carbon surface, which will favour the paracetamol adsorption on the resulting ACTT.

TABLE 1 HERE

2.2. Adsorption equipment and procedures

2.2.1. Batch adsorption.

The experimental methods used for the equilibrium and the kinetic studies were the same reported in previous works [37] and [38]. Paracetamol ($C_8H_9NO_2$ (99.5%) Sigma-Aldrich, molecular weight: 151.2 g mol^{-1}, melting point: 168-172ºC, solubility (20ºC): 14 g L^{-1}, pKa: 9.9) solutions were prepared with distilled water at different initial concentrations (1 – 20 mg L^{-1}). For the equilibrium tests, samples of 100 mL and doses

of 10.0 mg of dry activated carbon were put inside glass flasks and contacted in an orbital incubator (Gallenkamp, model INR-250) at 200 rpm equivalent stirring rate for 10 days. The adsorbate concentrations were determined by UV spectroscopy (λ_{max}: 243 nm) with an UV-Visible (Varian, Model Cary 1E) spectrophotometer. For the kinetic tests, paracetamol solutions (7 mg L^{-1}) were put in contact with activated carbon and agitated for different times with adsorbent doses of 10.0 mg. The temperatures for the experiments varied between 15 ºC and 35 ºC.

From the batch tests, the adsorption capacities at equilibrium, q_e (mg g^{-1}), were calculated as:

$$q_e = \frac{C_0 - C_e}{w} \quad (1)$$

where C_0 and C_e represent the initial and the equilibrium concentrations (mg L^{-1}) of the adsorbate in solution, and w is the adsorbent dose (g L^{-1}).

The experimental data for paracetamol adsorption at the equilibrium were fit using the adsorption isotherm model of Langmuir:

$$q_e = \frac{q_L \cdot K_L \cdot C_e}{1 + K_L \cdot C_e} \quad (2)$$

K_L is the equilibrium constant (L mg^{-1}), usually related to the enthalpy of adsorption, and q_L is the equilibrium concentration of the adsorbate (mg g^{-1}) on the solid phase corresponding to a complete coverage (adsorption capacity for a monolayer).

The adsorbed amount of paracetamol, q_t, in the kinetic tests was calculated as:

$$q_t = \frac{C_0 - C_t}{w} \quad (3)$$

where C_t (mg L^{-1}) represents the adsorbate concentration in the aqueous phase at time *t* (min).

The kinetic experimental results have been fitted by a hyperbolic equation previously used by us, [38] and [39], for smoothing the experimental curves, which will be helpful in avoiding noise during subsequent treatment of the experimental data:

$$q_t = \frac{a \cdot q_m \cdot t}{1 + a \cdot t} \quad (4)$$

$$\frac{dq_t}{dt} = \frac{a \cdot q_m}{(1 + a \cdot t)^2} \quad (5)$$

where *a* and q_m are empirical parameters related to the kinetic curve shape. q_m represents the asymptotic q_t value in the function at the set experimental conditions. Therefore, q_t tended to q_m at the maximum contact time in the kinetic test.

2.2.2. Column adsorption.

A diagram of the installation used in the adsorption study is showed in Fig. 2. The fixed bed adsorption tests were carried out in a thermostatized glass column (± 0.5 ºC), with internal diameter of 5mm and the length bed varied according to the amount of the activated carbon. A weighted amount of activated carbon was packed between two slices of inert quartz wool inside the column. The ability of the paracetamol to be adsorbed on the quartz fibers was discarded by a previous blank experiment with a quartz wool piece placed as adsorbent inside the column. Paracetamol solution was pumped downflow through the column at controlled flow rate using a peristaltic pump. The breakthrough curves were obtained by continuous monitoring of the effluent concentrations by UV spectrometry.

FIGURE 2 HERE

Before the column test was started, water (6 mL min^{-1}) was feed to the column for 20 minutes in order to remove the trapped air and to wet the activated carbon porosity. To minimize axial dispersion effects, the bed-length to particle diameter ratio (L_b/R_p) was larger than 20 for all experiments [40]. Two different sets of experiments were carried out to separate the effects from the concentration, temperature, flow rate and bed length changes. First, four tests were conducted to study the influence of the flow rate (4 and 8 mL min^{-1}) and the bed length (170 and 230 mg of activated carbon) on the adsorption kinetics at the experimental conditions of the central point of the design (DEO) as proposed in Fig. 3, i.e. 5 mg L^{-1} and 25 ºC.

FIGURE 3 HERE

Second, a DEO experimental design was used for minimizing the number of experiments required to study the influence of the temperature and the concentration, as showed in Fig. 3, while the solution flow and the activated carbon amount were set at 6 mL min^{-1} and 200 mg, respectively.

3. Mathematical models for the mass transfer

3.1. CP-LDF breakthrough process analysis

The linear driving force model (LDF) [41] has been widely applied to model the breakthrough profiles in activated carbons adsorption beds for several pollutants [42], [43] and [44]. It contemplates that the mass transfer rate at a given point of the bed is proportional to the difference between the current concentration of the solute on the adsorbent at a local level and that corresponding when the equilibrium with the bulk

phase is achieved. Under certain conditions, it can be considered that the adsorption fronts follow a constant pattern (CP) behavior, i.e. the front shape is unmodified while it propagates through the adsorption bed. Explicit equations for the breakthrough front can be derived for this CP-LDF [45].The equation of the CP-LDF model and the Langmuir isotherm was given by LeVan [46] in dimensionless form:

$$\frac{1}{1-R_{\mathrm{S}}}\mathrm{Ln}\left(\frac{1-{}^{C}/_{C_{\mathrm{i}}}}{\left({}^{C}/_{C_{\mathrm{i}}}\right)^{2}}\right)+1=N-N\cdot T \tag{6}$$

where N is the number of transfer units, and T and R_{S} are the throughput parameter and separation factor respectively, given by:

$$N=k_{\mathrm{i}}\frac{\rho_{\mathrm{b}}\cdot z\cdot q_{\mathrm{i}}}{u\cdot C_{\mathrm{i}}} \tag{7}$$

$$T=\frac{C_{\mathrm{i}}}{q_{\mathrm{i}}}\cdot\frac{1}{\rho_{\mathrm{b}}}\left(u\frac{t}{z}-\varepsilon_{\mathrm{b}}\right) \tag{8}$$

$$R_{\mathrm{S}}=\frac{1}{1+K_{\mathrm{L}}\cdot C_{\mathrm{i}}} \tag{9}$$

in these equations C_{i} is the inlet concentration, q_{i} is the equilibrium adsorbed amount at C_{i} from Langmuir equation, u is the superficial liquid velocity, z is the axial position in the bed, ε_{b} and ρ_{b} are the bed porosity and density, and t is the time. The intraparticle mass transfer coefficient, k_{i}, is given by:

$$k_{\mathrm{i}}=\frac{15\cdot D_{\mathrm{e}}}{R_{\mathrm{p}}^{2}}\cdot\frac{\varepsilon_{\mathrm{b}}}{1-\varepsilon_{\mathrm{b}}} \tag{10}$$

where R_p is the radius of the particle and D_e is the effective intraparticle diffusion coefficient, which is experimentally determined using the Reichenberg equation (detailed in 4.2.2. section).

The breakthrough curve equation obtained in working variables is:

$$t = t_s - \frac{1}{k_i}\left(1 + \frac{1}{1 - R_S}\mathrm{Ln}\frac{1 - {C}/{C_i}}{\left({C}/{C_i}\right)^{R_S}}\right) \quad (11)$$

where the stoichiometric time, t_s, is written as follows:

$$t_s = \frac{W \cdot q_i}{Q \cdot C_i} \quad (12)$$

being W the mass of the carbon and Q the volumetric flow rate.

3.2. Mass balance analysis

3.2.1. Physical assumptions.

The use of two mass transfer resistance models for adsorption is generally accepted as the best choice for describing the adsorption process in activated carbons [47]. A model that considers external-film and diffusion mass-transfers beside axial dispersion along the bed length has been used in this work to calculate the breakthrough profiles under varying operation conditions. The following assumptions are made in the sake of providing an adequate description of the operation of the column:

- Gradients in the concentration profiles of the adsorbate due to radial flow are accepted as negligible. They are excluded by a suitable design of the column (R_b>20 R_p).

- The process operates under isothermal conditions, being ensured by thermostatizing the column using a recirculate water bath.
- The activated carbon particles are treated as spherical and homogeneous in size and density.
- The axial velocity, v_z (m s^{-1}), is supposed to be constant and the occurrence of preferential paths is not considered.
- Mass transport between the bulk phase and the solid particle is described by the external-film mass-transfer coefficient, k_f (m s^{-1}) [48].
- Intraparticle mass transfer mainly controlled by surface diffusion, represented by an effective diffusion coefficient D_e (m^2 s^{-1}).

3.2.2. Fluid phase to external surface mass balance.

After assuming the aforementioned hypothesis, a generalized differential equation for the mass balance of the solute which flows through a fixed bed adsorber can be drawn:

$$\frac{\partial C_b}{\partial t} = -v_z \cdot \frac{\partial C_b}{\partial z} + D_z \cdot \frac{\partial^2 C_b}{\partial z^2} - k_f \cdot \frac{3}{R_p} \cdot \frac{(1-\varepsilon_b)}{\varepsilon_b} \cdot (C_b - C_p) \quad (13)$$

in this equation C_b is the bulk adsorbate concentration in the water flowing through the bed, C_p is the concentration in the particle external surface, and D_z is the axial dispersion coefficient. The terms of Eq. (13) account the phenomenon for the transient, convective, axial dispersion and external mass transfer across the boundary layer between the bulk and the external surface of the adsorbent, respectively.

The initial conditions and the boundary conditions at the both ends of the bed are:

t=0; z=0; C_p=0; C_b=0

391 t=0; $z>0$; $C_p=0$

392 t>0; $z=0$; $D_z \cdot \partial C_b/\partial z = v_z/\varepsilon_b \cdot (C_b - C_i)$

393 t>0; $z=L_b$; $\partial C_b/\partial z \frac{\partial C_b}{\partial z} = 0$

394 where L_b is the length of the fixed bed.

395 The external mass transfer coefficient as well as the axial dispersion coefficient were
396 calculated using the following correlation [49]:

397 $$k_f = \frac{D_l \cdot \left(2 + 0.644 \cdot Re^{1/2} \cdot Sc^{1/3}\right) \cdot \left(1 + 1.5 \cdot (1 - \varepsilon_b)\right)}{2 \cdot R_p} \quad (14)$$

398 Being *Re* and *Sc* the Reynolds and Schmidt numbers, and D_l the molecular diffusivity
399 for the solute (i.e., paracetamol in water $7 \cdot 10^{-10}$ m^2 s^{-1}).

400 $$Re = \frac{2 \cdot R_p \cdot v_z \cdot \rho_l}{\mu_l} \quad (15)$$

401 $$Sc = \frac{\mu_l}{D_l \cdot \rho_l} \quad (16)$$

402 $$D_z = D_l = \frac{1.326 \cdot 10^{-4}}{\mu_l^{1.14} \cdot V_b^{0.589}} \quad (17)$$

403 where ρ_l (1000 kg m^{-3}) and μ_l (0.00089 kg m^{-1} s^{-1}) are the density and viscosity of the
404 fluid through the column (for Eq (17) μ_l = 0.89 cP), and V_b (191 cm^3 mol^{-1}) is the molar
405 volume of the solute at its normal boiling point. V_b has been calculated using the
406 estimation formula proposed by Treybal [50].

407

408 **3.2.3. Mass balance within the particles.**

Since diffusion is considered to be predominant in the mass transfer through the micropore system of the activated carbon [47] and [51], the mass balance within a differential radial section of an adsorbent particle can be described by the following equation:

$$\varepsilon_p \cdot \frac{\partial q_r}{\partial t} = -\frac{1}{r^2} \cdot \frac{\partial (r^2 \cdot N_s)}{\partial r} \quad (18)$$

where ε_p is the particle porosity, q_r the adsorbed concentration at the radial r position in the spherical particle.

The diffusion molar flux N_s can be expressed according to the Fick's law:

$$N_S = -\left(D_e \cdot \frac{\partial q_r}{\partial r}\right) \quad (19)$$

As for the estimation of the effective diffusion coefficient, D_e, it has been detailed in the 4.2.2. section. Finally, the required initial and boundary conditions are:

t=0; $q_r = 0$

t>0; r=0; $\partial q_r / \partial = 0$

t>0; r=R_p; $Ns = k_f \cdot (C_b - C_p)$

In the approach proposed in this work, the surface concentrations profiles along the radius of the particle are averaged by means of the assumption of parabolic concentration profiles of the solute within the pores. This approximation has been found to be trustworthy when comparing these profiles with those obtained from the rigorous approach [52]. As a consequence of the parabolic concentration profile approximation, the mass balance equation can be simplified as follows:

$$Ns = 5 \cdot \frac{D_e}{R_p} \cdot \left(q|_{Cp} - \bar{q}\right) \quad (20)$$

$$\frac{\partial \bar{q}}{\partial t} = -\frac{15 \cdot D_e}{R_p^2} \cdot \left(q|_{Cp} - \bar{q}\right) \quad (21)$$

where $\bar{q}$ represents the mean concentration of solute adsorbed in the adsorbent particle and $q|_{Cp}$ stands for the adsorbed concentration at the solid external surface which is in equilibrium with C_p. Last, the boundary condition at the external surface of the particle requires that the diffusion flow entering must be equal to the molar transfer rate through the liquid film around the particle:

$$Ns = \frac{5 \cdot D_e}{R_p} \cdot \left(q|_{Cp} - \bar{q}\right) = k_f \cdot \left(C_b - C_p\right) \quad (22)$$

This equation allows to establishing the C_p value. This is possible because the adsorbed concentration $q|_{Cp}$ may be related to the fluid phase concentration C_p in that same location, at $r=R_p$, by an adequate adsorption equilibrium isotherm.

4. Results and discussion

4.1. Adsorption equilibrium

The equilibrium adsorption isotherms of paracetamol solutions at 15, 25 and 35 ºC are showed in Fig. 4. The isotherms resulted as type L of Giles classification [53] and the observed uptakes for low equilibrium PA concentration are close to the values reported for P-containing activated carbons prepared at 800º C [36] or activated carbons prepared by physical activation with CO_2 [22]. However, it is important to note that the paracetamol adsorption have been studied in the present work using one order of magnitude lower than that used in the reported works. At higher paracetamol

concentrations, lateral interaction between adsorbed species and/or multilayer adsorption may enhance the adsorbed amount by the activated carbon [20].

In our case, the increase on adsorption temperature produces a decrease in the paracetamol adsorbed amount, which suggests the exothermic nature of the adsorption process. The Langmuir adsorption parameters were calculated using a non-linear regression fitting procedure. The values of K_L, q_L and r^2 (determination coefficient) are showed in Table 2.

FIGURE 4 HERE

The free energy (ΔG), enthalpy (ΔH) and entropy (ΔS) changes were calculated by the following equations: the free energy change related to the equilibrium constant (Eq . 23), the Van't Hoff's (Eq. 24) for the enthalpy change, and the Gibbs-Helmholtz's (Eq. 25) to estimate the entropy change. The values obtained are showed in Table 2.

$$\Delta G = -RT \ln K_L \quad (23)$$

$$\frac{\partial \ln K_L}{\partial T} = \frac{\Delta H}{R \cdot T^2} \Rightarrow \ln K_L = \ln K_{L0} - \frac{\Delta H}{R \cdot T} \quad (24)$$

$$\Delta S = \frac{\Delta H - \Delta G}{T} \quad (25)$$

in these equations, R is the gas constant (8.31 J mol^{-1} K^{-1}), T is the absolute temperature (K), and K_{L0} is the pre-exponential factor, i.e., the value of K_L when T tends to infinite.

The negative values of ΔG from Eq. (23) indicate the spontaneity of the adsorption process. The average molar values of ΔG are quite influenced by the temperature.

TABLE 2 HERE

The low negative value of the enthalpy from the slope in the linear regression of Eq. (24) confirms the exothermic nature of the adsorption process. However, there are some studies that report the paracetamol adsorption process on activated carbons being endothermic [20] and [22]. These discrepancies are accountable to the higher paracetamol concentration used in those studies (> 100 mg L^{-1}), enabling the formation of dimers and micelles. When these agglomerations appear, the adsorption is favored as the temperature increases due to a lower amount of dimers in solution and an increased diffusion of the solution through the porosity of the activated carbon. This is not the case of the study showed in this paper, where the low concentrations do not favor the formation of dimers and micelles. Positive values of the adsorption entropy changes from Eq. (25) are coherent with a decrease of the freedom of the molecules in the fluid phase when they are adsorbed.

4.2. Kinetic study

4.2.1. Empirical model for the liquid phase adsorption.

The kinetic results obtained at three temperatures are showed in Fig. 5. It is clear that the adsorption rate and yield increase with increasing the temperature. This is due to the enhancement of diffusion rate of the solute through the porous structure. It can be observed (plot inset in Fig. 5a) that q_t-t curves for different temperatures intersect at long times, and the higher adsorption temperature is, the lower time to reach the equilibrium state is and the lower amount of paracetamol adsorbed in equilibrium is.

Table 3 compiles the fitting coefficients, whereas Fig. 5b presents the PA adsorption rate at different temperatures derived from Eq. (5). A sharp decrease in the adsorption rate is observed for the first minutes of contact time. This step corresponds to the surface coverage in the most available adsorption sites, probably on the more accessible and wider pores. A second adsorption stage runs for 3 h approximately with an intermediate decreasing rate. The last phase leads to the equilibrium concentrations, and could take extremely long times of contact time, in the range of several days.

FIGURE 5 HERE

4.2.2. Effective diffusion coefficients.

The effective diffusion coefficient (D_e) can be obtained from the data of PA adsorption rate obtained in the batch study according to the procedure given by Reichenberg [54]:

$$F(t) = \frac{q_t}{q_e} = 1 - \frac{6}{\pi^2}\sum_{n=1}^{\infty}\frac{1}{n^2}\exp\left(-\frac{n^2\pi^2}{R_p^2}D_e \cdot t\right) = 1 - \frac{6}{\pi^2}\sum_{n=1}^{\infty}\frac{1}{n^2}\exp(-n^2 \cdot B \cdot t) \quad (26)$$

where B is the time constant,

$$B = D_e \,\pi^2 \Big/ R_p^2 \quad (27)$$

and $F(t)$ is the fractional uptake (q_t/q_e) at time t. By applying the Fourier transform and integration, Reichenberg obtained the following approximation for F(t) <0.85.

$$B \cdot t = \left(\sqrt{\pi} - \sqrt{\pi - (\pi^2 \cdot F(t)/3)}\right)^2 \quad (28)$$

The values of the second member in Eq. (28), i.e. each observed value of $F(t)$, may be plotted vs t to distinguish between adsorption controlled by external or internal

diffusion. If it is linear and passes through the origin, then the adsorption rate is controlled by the diffusion within the particles. Otherwise, the adsorption may be also goberned by the film diffusion considered as a external mass transfer. The results are summarized in Table 3. The *B·t* plots for each adsorption temperature are shown in Fig. 6. The linearity of the plots ($r^2 > 0.976$) and the almost zero value of Y-intercept indicate that the mass-transfer process is controlled by the internal diffusion. From the slope of the slope of the B·t plot, effictive diffusion coeficients have been obtained at 15, 25 and 35º C. They have been termed heretofore as homogeneous diffusion coefficients, in clear contrast to those obtained considering that the difussion coefficient varies with the surface coverage of PA, which are referred as heterogeneous diffusion conefficients. The relationship between heterogeneous D_e and surface coverage has been reflected by using the Vermeulen equation [55]:

FIGURE 6 HERE

$$\frac{q_t}{q_e} = \left[1 - \exp\left(\frac{-D_e \pi^2 t}{R_p^2}\right)\right]^{0.5} \quad (29)$$

$$D_e = \frac{-R_p^2}{\pi^2 t} \mathrm{Ln}\left[1 - \left(\frac{q_t}{q_e}\right)^2\right] \quad (30)$$

The hyperbolic Eq (4) has been used for the estimation of q_t. Eq (4) and (30) have been employed for establishing the relationship between the diffusion coefficient and the surface coverage, i.e. the adsorbed amount of paracetamol. First, D_e for each *t* is estimated from (30), then, the obtained data were fitted to an exponential empirical equation:

$$D_e = b \cdot \exp\left(\frac{c}{t+d}\right) \quad (31)$$

b, *c*, and *d* are empirical parameters. The hyperbolic Eq (4) can be combined with (31) in order to obtain an expression which relates the diffusion coefficient with q_t:

$$D_e = b \cdot \exp\left(\frac{c}{\left(\frac{q_t}{a}\right)/(q_e - q_t) + d}\right) \quad (32)$$

The fitting of D_e vs q_t was conducted using contact times higher than 200 min to avoid the underestimation of D_e at low contact times, where the wetting process of the initially dry micropores hinders the mass transfer of the adsorbate through the particle. Table 3 compiles the resulting fitting coefficients.

FIGURE 7 HERE

Fig. 7 presents the relationship between the effective diffusion coefficient and the adsorbed amount of paracetamol (i.e. PA surface coverage) for a given initial concentration (7 mg L^{-1}) and different temperatures. As expected the calculated curves corroborate that an increase in the temperature of the batch adsorption experiment are answered by an overall increase in the value of the diffusion coefficients. As for the dependence of diffusion with the adsorbed amount of PA, D_e values decrease with the surface coverage (or time) due to the depletion of the available free adsorption sites that are necessary to allocate the adsorbed PA molecules that are diffusing over the surface. This decrease of the diffusion coefficient can also be explained in terms of the wide pore structure distribution of the pore network and the heterogeneity of the surface chemistry of the activated carbon, which will render not only different energies of interaction between the adsorbate and the adsorbent depending on the surface coverage of PA over the carbon surface, but also a different mobility of the adsorbed PA

559 molecule on the pore network,. Thus, as the adsorption phenomenon proceeds (long
560 times), paracetamol will be adsorbed first in the more energetically favorable and
561 accessible adsorption sites at a fast rate. When the most favored sites are fully covered
562 by PA, the mass transport becomes progressively controlled by a slower diffusion of the
563 paracetamol into the less energetically favorable and isolated adsorption sites.

564 **TABLE 3 HERE**

565

566

567 **4.3. Column adsorption studies**

568 Fig. 8 presents a scheme of a breakthrough curve for paracetamol adsorption on ACTT,
569 where the procedure followed for the calculation of the breakthrough curve by solving
570 the mass balance to the fixed-bed adsorber is also detailed. The mathematical calculus
571 was carried out applying the finite differences method with 75 points to the length
572 variable (*z*) in Eq. (13) of the mass balance for the fixed-bed adsorber. For each *i* point,
573 first C_{pi} is determined from Eq (22), then $\partial \overline{q_i}/\partial t$ is estimated from Eq (21) using C_{pi},
574 the Langmuir constants and the heterogeneous diffusion coefficient determined from
575 batch adsorption experiments and Eq (2) and (32). Third, since Eq (13) have been
576 discretized in the *z* variable following the finite differences method [56], $\partial Cb_i/\partial t$ can
577 be calculated by evaluation of the convective and dispersive flows from the *i-1* point
578 and dispersive flow from the *i+1* point, the convective flow from *i* to the *i+1* point, and
579 the flow through the stationary liquid film over the carbon particle, which is estimated
580 using the freshly determined value of C_{pi}. The proper boundary conditions are
581 considered in the case of 1st and 75th point. Finally, a 4th order Runge-Kutta method is
582 used for solving in time $\partial \overline{q_i}/\partial t$ and $\partial Cb_i/\partial t$ for the 75 points. The C_b value at the 75th

583 point, the one localized at the end of the fixed bed, is stored and used for obtaining the
584 breakthrough profile.

585 It is important to note that the kinetic and equilibrium adsorption parameters obtained in
586 batch system, i.e. adsorption isotherm constants and the effective diffusion coefficient,
587 have been used for solving the mass balance equations that allow the prediction of the
588 breakthrough profile. Note that the solution of these equations allows the determination
589 of the time for the breakthrough appearance or bed service time (BST), which is
590 stablished as the time at what the outlet concentration reach the C/C_i = 0.05 value, and
591 the shape of the breakthrough profile, which is related to the height of the mass transfer
592 zone (H_{MTZ}). These are actually critical parameters for determining the operation and
593 the dynamic response of an activated carbon when used as adsorbent for an adsorption
594 bed that cannot be directly determined from batch adsorption experiments. In simple
595 terms, the breakthrough time is proportional to the capacity of the adsorbent, while
596 inversely related to the H_{MTZ} value. For a given inlet concentration, the adsorption
597 capacity of the adsorbent can be determined if its adsorption isotherm is established.
598 Contrariwise, the height of mass transfer zone does not keep a direct relationship to any
599 specific kinetic parameter, and it results from the interaction between the
600 hydrodynamics of the experimental set-up and the surface properties (surface chemistry,
601 pore structure) of the adsorbent [57]. Since breakthrough time and therefore bed service
602 time are dependent on both H_{MTZ} and adsorption capacity, and there is no direct
603 relationship between H_{MTZ} and the kinetic and thermodynamic batch adsorption
604 parameters, the numerical solving of the mass balance equations detailed here is
605 proposed for predicting them.

606 **FIGURE 8 HERE**

607 The validity of some of the assumptions made in section 3.2.1 have been checked by
608 analyzing the dimensionless numbers that dictate the dominating processes during the
609 operation of the fixed bed adsorber. Table 4 compiles the experimental values of the
610 adsorbent and the bed that have been used for this purpose, along with the values of the
611 mentioned dimensionless numbers concerned. The Reynolds values (Re) between 0.97
612 and 1.96 indicate that a laminar flow regime is governing in the fixed bed, and that
613 liquid flow through the column is meanly produced by convection, hence the Schmidt
614 number (Sc) was higher than 12.71 for all the column experiments. The high values of
615 Peclet number (Pe), between 1931 and 3778, as well as the low axial dispersion
616 coefficient ($7 \cdot 10^{-10}$ m^2 s^{-1}, estimated from equation (17)) suggest that the influence of
617 this phenomenon on the column behavior is negligible. Values of the Biot number (Bi)
618 and the mass transfer coefficient (k_f) are also high, pointing out the absence of limited
619 mass transfer through the stationary layer of liquid around the particles of the adsorbent.

620

621 **TABLE 4 HERE**

622

623 Fig. 9 to 12 show the breakthrough profiles obtained for the paracetamol adsorption in
624 the activated carbon fixed-bed under different operating conditions. All the
625 experimental breakthrough curves follow the typical S-shaped curve for column
626 operation with favorable adsorption isotherms [58]. In all the curves, the experimental
627 data are identified by symbols, whereas the breakthrough curves calculated by CP-LDF
628 are plotted using discontinuous line and those obtained from the solution of the
629 numerical model with heterogeneous diffusion coefficient proposed in this work have
630 been represented by continuous lines. The profiles are reported in terms of treated

631 volume for easing the comparison among results obtained using different experimental
632 conditions (flow rate, inlet concentration, temperature…). It can be observed in Fig. 9-
633 12 how the thermodynamic and kinetic parameters obtained in stirred tank and then
634 introduced in the numerical solution proposed in this work for the mass balance to the
635 fixed-bed adsorber can satisfactorily explain the experimental curves when the
636 heterogeneous effective diffusion coefficient approach is considered. In contrast, CP-
637 LDF could not provide an accurate description of the breakthrough profile. The reasons
638 will be discussed in detail above.

639

640 **4.3.1. Effect of the flow rate.**

641 The experiments displayed in Fig. 9 were conducted at variable flow rates to establish
642 the possible influence of mass transfer in the film of stationary liquid that surrounds the
643 particle. The rest of the experimental conditions were those used for the central point,
644 i.e. 25 ºC, 5 mg L^{-1} of paracetamol at the column inlet and 200 mg of activated carbon.
645 It was found that the variation of the flow rate has a negligible impact on the shape of
646 the breakthrough curves, confirming the absence of external mass transfer control, as
647 predicted from the Biot numbers in Table 4. This finding was further corroborated by
648 simply solving the mass balance to the fixed bed and the carbon particle proposed in
649 3.2.2. and 3.2.3. sections while removing the consideration of external mass transfer
650 (thus, $C_p = C_b$). The obtained profile was identical to that obtained when the mass
651 balance was solved upon consideration of external mass transfer in the liquid film.

652

653 **FIGURE 9 HERE**

654

655 **4.3.2. Effect of the amount of activated carbon.**

656 The effect of axial dispersion was analyzed by carrying out experiments at 25 ºC, PA
657 concentration of 5 mg L^{-1}, flow rate of 6 mL min^{-1} and different bed lengths (2.6-3.2
658 cm). As observed in Fig. 10, the breakthrough time is affected by the amount of
659 activated carbon. The behavior of the breakthrough profile at different lengths, which
660 shows a similar shape no matter the chosen bed length, leads to the conclusion that it
661 does not exist any back mixing or axial dispersion problem in the column. This assert is
662 in accordance with that drawn from the high values of the Peclet number showed in
663 Table 4, and was again confirmed by the absence of any relevant difference when the
664 mass balance in 3.2.2 was solved without including the axial dispersion term. Therefore,
665 and under the operating conditions selected for this work, the mass balance to the small
666 column can be solved without considering axial dispersion and external mass transfer
667 control, and consequently the numerical solution can be simplified reflecting these
668 conclusions. Note that, under such conditions, the CP-LDF can theoretically be used for
669 describing the behavior of the fixed-bed adsorber [41]. Nevertheless, by following the
670 approach proposed in this work the breakthrough profiles have been modeled obtaining
671 a much higher accuracy in the description of the experimental curves, as can be seen
672 along Fig. 9 to 12.

673

674 **FIGURE 10 HERE**

675

676

677 **4.3.3. Effect of adsorption temperature and PA concentration.**

678 Fig. 11a shows the breakthrough curves for the PA adsorption at different temperatures,
679 in all cases the inlet concentration was kept at 5 mg L^{-1}, the flow rate at 6 mL min^{-1} and
680 a bed of 200 mg of activated carbon was used. It can be seen that the breakthrough time
681 ($C/C_i \approx 0.05$) decreased when temperature increases, while the saturation times ($C/C_i \approx$
682 0.95) were higher for those runs performed at lower temperature, and the height of the
683 mass transfer zone decreased a 20% when raising the temperature from 15 to 35º C.
684 These modifications are reflecting the higher values for the diffusion coefficients and
685 the lower paracetamol adsorption capacities at higher temperatures that were already
686 found in the batch study.

687 The effect of the inlet concentration of paracetamol on the breakthrough profiles has
688 also been analyzed and featured in Fig. 11b. Again, the expected behavior is found
689 when concentration decreases, finding a great increase the breakthrough time, a lower
690 adsorption capacity and similar value of H_{MTZ}. For all the experimental conditions
691 tested in this work, the worse profile simulation was found for the experiment
692 conducted at C_i = 3 mg L^{-1}. The main reason of the inaccurate prediction of the
693 breakthrough time seems to be the increase of the uncertainty in the determination of the
694 adsorption capacity of the ACTT at low concentrations of PA from the batch study.

695 **FIGURE 11 HERE**

696 Finally, in order to be useful an adsorption model for fixed-bed adsorbers should be able
697 to truthfully predict the breakthrough behavior at different conditions than those used
698 for the estimation of the adsorption parameters. In this sense, Fig. 12 shows the
699 breakthrough curves at 18 and 32 ºC, respectively, using 6 mL min^{-1}, 200 mg of
700 activated carbon and 4 and 6 mg L^{-1} of paracetamol. Since the thermodynamic and

kinetic studies were carried out at 15, 25 and 35 ºC, the thermodynamic and kinetic adsorption parameters values fed to the models were estimated using a linear interpolation method. A good concordance was found with the mathematical solution of the mass balance and the q_t-dependent D_e, while CP-LDF failed to reproduce the bed behavior. It has been found once more that the curves for the higher concentration at the inlet are better described than those obtained using low concentration of paracetamol, highlighting the reliance of the accuracy of the proposed model in a precise determination of the adsorption isotherm during the batch study.

FIGURE 12 HERE

4.3.4. Design parameters and models comparison.

Table 5 presents the experimental values of adsorbed paracetamol amount (q_{exp}) as well as the BST and H_{MTZ} obtained for all the tested operational conditions. It can be seen that the adsorbed amounts ranged between 68 and 89 mg of PA per gram of activated carbon, while the low values of the H_{MTZ} results in an actual use of 60 to 80% of the available paracetamol remediation capacity before the PA outlet concentration reached the selected limit. As for the calculus of the design parameters, there are only few samples in the literature about using the adsorption parameters obtained from the batch studies in order to estimate the fixed bed behavior [51 o 59] of an adsorbent. In this study, the CP-LDF and the numerical solution of the mass balances have been employed for that purpose, and the resulting breakthrough profiles for each model have been shown along with the experimental data in Fig.s 9 - 12. Table 5 compiles the estimated design parameters for every tested operation conditions. It can be seen that the paracetamol adsorptivities calculated using the mass balance procedure are very close to

725 those obtained from the experimental breakthrough profiles. Similarly, H_{MTZ} and BST
726 are accurately predicted for all the tested experimental conditions. Furthermore, the high
727 values of r^2 indicate that the proposed model can reproduce fairly well not only BST
728 and H_{MTZ}, but also most of the experimental breakthrough profile. Inversely, the CP-
729 LDF model cannot be used for a satisfactory determination of the operation behavior of
730 the fixed bed adsorbed. The lack of accuracy undeniably relies on the approach adopted
731 for estimating the diffusivity, since CP-LDF cannot reflect the dependence of the
732 diffusivity coefficient with adsorbed amount that is known to be not necessarily
733 constant in rapid small-scale column tests [18], especially in the case of the highly
734 heterogeneous pore structure of activated carbons.

735 **TABLE 5 HERE**

736 **5. Conclusions**

737 Activated carbon has been prepared by chemical activation of olive stones with
738 phosphoric acid, obtaining a porous carbon material with a well-developed porous
739 structure and specific surfaces area close to 1000 $m^2\ g^{-1}$. Adsorption of paracetamol (a
740 model emerging pollutant) at low concentration (0.3 to 10 mg L^{-1}) and mild
741 temperatures (from 15 to 35º C) has been studied using discontinuous (batch) and flow
742 column adsorption experiments. The adsorption isotherm is well described using the
743 Langmuir model, showing adsorption capacities of ca. 100 mg g^{-1} at 9 mg L^{-1}, a value
744 that is only slightly influenced by temperature. Kinetic studies in discontinuous batch
745 experiments have been used for the estimation of effective homogeneous and
746 heterogeneous diffusion coefficients. In the latter case, an empirical equation has been
747 drawn to relate the heterogeneous diffusion coefficient with the surface coverage of
748 paracetamol. The effectiveness of the H_3PO_4-activated carbon for paracetamol removal
749 has also been studied using rapid small-scale column experiments. The activated carbon

showed high bed service times and reduced heights of the mass transfer zone due to the favorable adsorption of paracetamol on its surface. The effects of operational variables (temperature, flow rates, fixed-bed length and inlet concentration) have been analyzed using a design of experiments.

The most important finding in this work was the possibility of accurately modeling the breakthrough behavior of the fixed-bed adsorber by using the kinetic and thermodynamic parameters obtained from the batch experiments. Inappropriate handling of the data obtained from the batch experiments and the use of simplified models that considers a constant diffusion coefficient like CP-LDF do not allow a trustworthy prediction of the design parameters of the column, like BST or H_{TMZ}. In contrast, by using the adequate experimental and boundary conditions, mathematical tools, model considerations and a diffusion coefficient related to the surface coverage of the pollutant, it is possible to attain from simple batch experiments a precise knowledge of the performance of a given adsorbent in column adsorption, which allows an accurate prediction of the breakthrough profile, BST and H_{MTZ}.

Acknowledgments

We gratefully thank Junta de Andalucía (P09-FQM-5156) and Spanish Ministry of Economy and Competitiveness (MINECO) (Project CTQ2012-36408) and FEDER for financial support. RRR acknowledges the financial support of MINECO through a JdC grant (JCI-2012-12664).

References

[1] T.A. Ternes, Ocurrence of drug in German sewage treatment plants and rivers. Water Res. 32 (1998) 3245-3260.

774 [2] R. Hirsch, T. Ternes, K. Haberer,K.L. Kratz, Occurrence of antibiotics in the aquatic
775 environment. Sci. Total Envoron. 225 (1999) 109-118.

776 [3] S.A. Snyder, P. Westerhoff, Y. Yoon, D.L. Sedlak, Pharmaceuticals, personal care
777 products, and endocrine disruptors in water: Implications for water treatment. Eviron.
778 Eng. Sci. 20 (2003) 449-469.

779 [4] M. Carballa, F. Omil, J.M. Lema, M. Llompart, C. García-Jares, I. Rodríguez, M.
780 Gomez, T. Ternes, Behavior of pharmaceuticals, cosmetics and hormones in a sewage
781 treatment plant. Water Res. 38 (2004) 2918-2926.

782 [5] S. Suárez, M. Carballa, F. Omil, J.M. Lema, How are pharmaceutical and personal
783 care products (PPCPs) removed from urban wastewater?. Rev. Environ. Sci. Biotechnol.
784 7 (2008) 125-138.

785 [6] B. Kaspryzk-Hordern, R.M. Dinsdale, A.J. Guwy, The removal of pharmaceuticals,
786 personal care products, endocrine disruptors and illicit drugs during wastewater
787 treatment and its impact on the quality of receiving water. Water Res. 43 (2009) 363-
788 380.

789 [7] M. Petrovic', G. Susana, D. Barceló, Analysis and removal of emerging
790 contaminants in wastewater and drinking water. Trends Anal. Chem. 22 (2003) 685-
791 696.

792 [8] C. Fernández, M. González-Doncel, J. Pro, G. Carbonell, J.V. Tarazona, Ocurrence
793 of pharmaceutically active compounds in surface waters of the henares-jarama-tajo river
794 system (Madrid, spain) and a potential risk characterization. Sci. Total Environ. 408
795 (2010) 543-551.

796 [9] W. Chen, R. Parette, J. Zou, F.S. Cannon, B.A. Dempsey, Arsenic removal by iron-
797 modified activated carbon. Water Res. 41 (2007) 1851–1858.

798 [10] R. Parette, F.S. Cannon, The removal of perchlorate from groundwater by activated
799 carbon tailored with cationic surfactants. Water Res. 39 (2005) 4020–4028.

800 [11] P. Hou, F.S. Cannon, N.R. Brown, T. Byrne, X. Gu, C.N. Delgado, Granular
801 activated carbon anchored with quaternary ammonium/epoxide-forming compounds to
802 enhance perchlorate removal from groundwater. Carbon 53 (2013) 197–207.

803 [12] C. Moreno-Castilla, Adsorption of organic molecules from aqueous solutions on
804 carbon materials. Carbon. 42 (2004) 83-94.

805 [13] J.J.M. Órfão, A.I.M. Silva, J.C.V. Pereira, S.A. Barata, I.M. Fonseca, P.C.C. Faria,
806 M.F.R. Pereira Adsorption of a reactive dye on chemically modified activated
807 carbons—Influence of pH. J. Colloid Interface Sci. 296 (2006) 480–489.

808 [14] Hsieh, Chien-To, Hsisheng Teng, Influence of Mesopore Volume and Adsorbate
809 Size on Adsorption Capacities of Activated Carbons in Aqueous Solutions. Carbon
810 38(2000) 863–869.

811 [15] A.M. Redding, F.S. Cannon, The role of mesopores in MTBE removal with
812 granular activated carbon. Water Res. 56 (2014) 214–224.

813 [16] M.J. Greenwald, A.M. Redding, F.S. Cannon, A rapid kinetic dye test to predict the
814 adsorption of 2-methylisoborneol onto granular activated carbons and to identify the
815 influence of pore volume distributions. Water Res. 68 (2015) 784–792.

816 [17] J.C. Crittenden, J.K. Berrigan, D.W. Hand, Design of rapid small-scale adsorption
817 test for a constant diffusivity. J. Water Pollut. Control Fed. 58 (1986) 312–319.

818 [18] J.C. Crittenden, J.K. Berrigan, D.W. Hand, B. Lykins, Design of Rapid Fixed-Bed
819 Adsorption Tests for Nonconstant Diffusivities. J. Environ. Eng.113 (1987) 243–259.

820 [19] L. Cummings, R.S. Summers, Using RSSCTs to predict field-scale GAC control of
821 DBP formation. J. Am. Water Works Assn. 86 (1994) 88-97.

822 [20] A.P. Terzyk, , G. Rychlicki, The influence of activated carbon surface chemical
823 composition on the adsorption of acetaminophen (paracetamol) in vitro, The
824 temperature dependence of adsorption at the neutral pH. Colloids and Surfaces, 163
825 (2000) 135-150.

826 [21] I. Cabrita, B. Ruiz, A.S. Mestre, I.M. Fonseca, A.P. Carvalho, C.O. Ania, Removal
827 of an analgesic using activated carbons prepared from urban and industrial residues.
828 Chem. Eng. J. 163 (2010) 249-255.

829 [22] L.M. Cotoruelo, M.D. Marqués, A. Leiva, J. Rodríguez-Mirasol, T. Cordero,
830 Adsorption of oxygen-containing aromatics used in petrochemical, pharmaceutical and
831 food industries by means of lignin based active carbons. Adsorption 17 (2011) 539-550.

832 [23] M. Galhetas, A.S. Mestre, M.L. Pinto, I. Gulyurtlu, H. Lopes, A.P. Carvalho, Chars
833 from gasification of coal and pine activated with K_2CO_3: Acetaminophen and caffeine
834 adsorption from aqueous solutions. Chem. Eng. J. 433 (2014) 94-103.

835 [24] E. González-Serrano, T. Cordero, J. Rodríguez-Mirasol, L. Cotoruelo, J.J.
836 Rodríguez, Removal of water pollutants with activated carbons prepared from H_3PO_4
837 activation of lignin from kraft black liquors. Water Res. 38 (2004) 3043-3050.

838 [25] J.M. Rosas, , J. Bedia, J. Rodríguez-Mirasol, T. Cordero, HEMP-derived activated
839 carbon fibers by chemical activation with phosphoric acid. Fuel 88 (2009) 19-26.

840 [26] M. Jagtoyen, F. Derbyshire, Activated carbons from yellow poplar and white oak
841 by H_3PO_4. Carbon. 36 (1998) 1085-97.

842 [27] S. Brunauer, P.H. Emmett, E. Teller, Adsorption of gases in multimolecular layers.
843 J. Am. Chem. Soc 60 (1938) 309-319.

844 [28] K. Kaneko, C. Ishii Superhigh surface area determination of microporous solid.
845 Colloids Surfaces 67 (1992) 203-212.

846 [29] K. Kaneko, C. Ishii, M. Ruike, H. Kuwabara, Origin of superhigh surface area and
847 microcrystaline graphitics structures of activated carbon. Carbon. 30 (1992) 1075-1088.

848 [30] K. Kaneko, Determination of pore size and pore distribution. I. Adsorbents and
849 catalysts. J. Membr. Sci. 96 (1994) 59-89.

850 [31] M.M. Dubinin, E.D. Zaverina, L.V. Radushkevich, Sorption and structure of active
851 carbons. I. Adsorption of organic vapors. J. Phys. Chem. [URSS] 21 (1947) 1351-1362.

852 [32] J. Bedia, J.M. Rosas, J. Márquez, J. Rodríguez-Mirasol, T. Cordero, Preparation
853 and characterization of carbon based acid catalysts for the dehydration of 2-propanol.
854 Carbon 47 (2009) 286-294.

855 [33] J.M. Rosas, R. Ruiz-Rosas, J. Rodríguez-Mirasol, T. Cordero, Kinetic study of the
856 oxidation resistance of phosphorus-contining activated carbons. Carbon 50 (2012)
857 1523-1537.

858 [34] J.M. Rosas , J. Rodríguez-Mirasol, T. Cordero, NO reduction on carbon-supported
859 chromium catalysts. Energy Fuels. 24 (2010) 3321-3328.

[35] J. Bedia, J.M. Rosas, J. Rodríguez-Mirasol, T. Cordero, Pd supported on mesoporous activated carbons with high oxidation resistance as catalyst for toluene oxidation. Appl. Catal., B 94 (2010) 8-18.

[36] M. Wiśniewski, A. Pacholczyk, A.P. Terzyk, G. Rychliki, New phosphorus-containing spherical carbon adsorbents as promising materials in drug adsorption and relase. J. Colloid Interface Sci. 354(2011) 891-984.

[37] L.M. Cotoruelo, M.D. Marqués, F.J. Díaz, J. Rodríguez-Mirasol, T. Cordero, Activated carbons for lignin: Their application in liquid phase adsorption. Sep. Sci. Technol. 42 (2007) 3363-3389.

[38] L.M. Cotoruelo, M.D. Marqués, J. Rodríguez-Mirasol, J.J. Rodríguez, T. Cordero, Lignin-based activated carbons for adsorption of sodium dodecylbenzene sulfonate: Equilibrium and kinetics studies. J. Colloid Interface Sci. 332 (2009) 39-45.

[39] L.M. Cotoruelo , M.D. Marqués, F.J. Díaz, J. Rodríguez-Mirasol, T. Cordero, Equilibrium and kinetics study of congo red adsorption onto lignin-based activated carbons. Transp. Porous Media. 83 (2010) 573-590.

[40] N.S. Raghavan, D.M. Ruthven Numerical simulation of a fixed-bed adsorption column by the method of orthogonal collocations. AIChE J. 29 (1983) 922-925.

[41] E. Glueckauf, J.I. Coates, The influence of incomplete equilibrium on the front boundary of chromatograms and the effectiveness of separation, J. Chem. Soc. (1947) 1315–1321-

[42] T. Cheng, Y. Jiang, Y. Zhang, S. Liu, Prediction of breakthrough curves for adsorption on activated carbon fibers in a fixed bed. Carbon. 42 (2004) 3081-3085.

882 [43] A. Patton, B.D. Crittenden, S.P. Perera, Use of the linear driving force
883 approximation to guide the design of monolithic adsorbents. Chem. Eng. Res. Des. 82
884 (2004) 999–1009.

885 [44] N. Qi, W.S. Appel, M.D. LeVan, Adsorption dynamics of organic compounds and
886 water vapor in activated carbon beds. Ind. Eng. Chem. Res., 45 (2006) 2303–2314

887 [45] S. Sircar, J.R. Hufton, Why does the linear driving force model for adsorption
888 kinetics work?. Adsorption, 6 (2000) 137–147.

889 [46] D. LeVan, Asymptotic fixed bed behaviour: proportionate and constant patterns.
890 In: Rodriguyes, A.E., LeVan, D., Tondeur, D. (Eds.), Adsorption; Science and
891 Technology. Kluwer academic publishers, Dordrecht, The Netherlands, 1989, pp. 149-
892 168.

893 [47] H. Moon, W.K. Lee, Intraparticle diffusion in liquid-phase adsorption of phenols
894 with activated carbon in finite batch adsorber, J. Colloid Interface Sci. 96 (1983) 162–
895 171.

896 [48] A.P. Mathews, J.R. Weber, J. Walter, Effects of external mass transfer and
897 intraparticle diffusion on adsorption in slurry reactors, AIChE. Symp. Ser. 73 (1977)
898 91–98.

899 [49] V. Gnielinski, Equation for calculating the heat and mass transfer in packed beds of
900 spheres at medium and large Peclet number (Gleichungen zur Berechnung des
901 Warmeund Stoffaustausches in durchstromten ruhenden Kugelschuttungen bei mitteren
902 und grossen Pecletzhlen). Verf. Tech 12 (1978) 363-366.

903 [50] R.E: Treybal, Operaciones de trasnsferencia de masa (2nd ed). 858p. Mc Graw
904 Hill ed, 1988, ISBN 968-6046-34-8.

905 [51] A.I. Liapis, D.W.T. Ripping, The simulation of binary adsorption in activated
906 carbon colums using estimates of diffusional resistance within the carbon particles
907 derived from batch experiments. Chem. Eng. Sci. 33 (1978) 593-600.

908 [52] R.T. Yang, R.T. Gas separation by adsorption processes. Butterworths, BostonUK
909 Imperial College, 1987.

910 [53] C.H. Giles, T.H. MacEwan, S.N. Nakhwa, D. Smith, Studies in adsorption. Part XI.
911 A system of classification of solution adsorption isotherms, and its use in diagnosis of
912 adsorption mechanisms and in measurement of specific surface areas of solid. J. Chem.
913 Soc. (1960) 3973-3993.

914 [54] D. Reighenberg, Properties of Ion-Exchange resins in relation to their structure. III.
915 Kinetics of exchange. J. Am. Chem. Soc. 75 (1953) 589-597.

916 [55] T. Vermeulen, Theory of Irreversible and Constant-Pattern Solid Diffusion. Ind.
917 Eng. Chem. 45 (1953) 1664-1670.

918 [56] K.J. Beers, Numerical Methods for Chemical Engineering: Applications in
919 MATLAB. Cambridge University Press, 2006.

920 [57] D.M. Ruthven, Principles of adsorption and adsorption processes. 464p. Jhon
921 Wiley & Sons, 1984.

Table 1. Physico-chemical properties of ACTT.

Structural properties							Surface composition (XPS)			
A_{BET} ($m^2\ g^{-1}$)	A_t ($m^2\ g^{-1}$)	V_p ($cm^3\ g^{-1}$)	V_{mes} ($cm^3\ g^{-1}$)	V_t ($cm^3\ g^{-1}$)	V_{DR} ($cm^3\ g^{-1}$)	A_{DR} ($m^2\ g^{-1}$)	C (%w)	O (%w)	P (%w)	N (%w)
990	280	0.91	0.43	0.36	0.22	550	85.1	8.8	5.7	0.4

Table 2. Parameters obtained from equilibrium / thermodynamics study

Temperatures (°C)	Langmuir isotherm parameters			Thermodynamic parameters				
	q_L (mg g^{-1})	K_L (L mg^{-1})	r^2	ΔG (kJ mol^{-1})	ΔH (kJ mol^{-1})	K_{L0} (L mg^{-1})	r^2	ΔS (J mol^{-1} K^{-1})
15	108.3	1.33	0.978	-29.2				41.3
25	98.4	1.13	0.982	-29.9	-17.3	$9.856 \cdot 10^{-7}$	0.962	42.3
35	92.8	0.83	0.984	-30.1				41.5

Table 3. Parameters obtained from the kinetic study

Temperature (ºC)	15	25	35
Hyperbolic equation			
a (s^{-1})	$5.53 \cdot 10^{-5}$	$8.59 \cdot 10^{-5}$	$1.69 \cdot 10^{-4}$
q_m (mg g^{-1})	59.83	57.85	53.16
q_e (mg g^{-1})	57.61	55.89	53.05
r^2	0.9907	0.9910	0.9887
Homogeneous diffusion coefficient			
D_e (m^2 s^{-1})	$1.6 \cdot 10^{-14}$	$2.5 \cdot 10^{-14}$	$4.0 \cdot 10^{-14}$
Heterogeneous diffusion coefficient			
b (m^2 s^{-1})	$1.18 \cdot 10^{-15}$	$1.55 \cdot 10^{-15}$	$2.32 \cdot 10^{-15}$
c (s)	387	298	202
d (s)	145	106	67
r^2	0.9995	0.9993	0.9983

Table 4. Operation variables for the adsorption column process.

T (ºC)	W (mg)	Q (mL min^{-1})	C_i (mg L^{-1})	L_b (cm)	ε_b	Re	Sc	Pe	Bi	k_f x10^3 (m s^{-1})
15	200	6	4.9	2.9	0.729	1.45	12.71	2896	858	2.03
18	200	6	3.9	2.8	0.719	1.47	12.71	2834	760	2.06
18	200	6	5.8	2.9	0.729	1.45	12.71	2896	1026	2.03
25	200	6	6.7	2.9	0.729	1.45	12.71	2896	1254	2.03
25	200	6	4.9	2.8	0.719	1.47	12.71	2834	997	2.06
25	200	6	2.9	2.9	0.729	1.45	12.71	2896	690	2.03
25	200	4	4.9	2.8	0.729	0.97	12.71	1931	896	1.85
25	200	8	4.8	2.8	0.719	1.96	12.71	3778	1054	2.21
25	170	6	4.9	2.6	0.743	1.43	12.71	2547	961	1.99
25	230	6	4.9	3.1	0.708	1.50	12.71	3186	1012	2.09
32	200	6	3.9	2.9	0.729	1.45	12.71	2896	940	2.03
32	200	6	5.9	2.9	0.729	1.45	12.71	2896	1237	2.03
35	200	6	4.9	2.9	0.729	1.45	12.71	2896	1142	2.03

Table 5. Experimental and design parameters for breakthrough curves.

T (ºC)	W (mg)	Q (mL min^{-1})	C_i (mg L^{-1})	*EXPERIMENTAL*			*MASS BALANCE*				*CP-LDF*			
				q_{exp}* (mg g^{-1})	*BST* (min)	H_{MTZ} (cm)	q_{cal}* (mg g^{-1})	*BST* (min)	H_{MTZ} (cm)	r^2	q_{cal}* (mg g^{-1})	*BST* (min)	H_{MTZ} (cm)	r^2
15	200	6	4.9	87.3	365	1.14	90.2	348	1.33	0.9952	92.2	327	1.69	0.9874
18	200	6	3.9	79.1	460	0.93	83.1	420	1.23	0.9638	85.9	433	1.46	0.9967
18	200	6	5.8	86.0	311	1.09	89.4	302	1.24	0.9868	90.6	271	1.70	0.9937
25	200	6	6.7	88.4	278	1.03	83.9	262	1.14	0.9965	85.5	238	1.55	0.9543
25	200	6	4.9	81.1	353	1.02	80.3	338	1.11	0.9981	82.4	335	1.38	0.9766
25	200	6	2.9	69.8	555	0.91	72.7	490	1.24	0.9790	74.6	600	1.16	0.9981
25	200	4	4.9	77.1	632	0.62	80.8	605	0.78	0.9304	82.3	650	0.89	0.9950
25	200	8	4.8	78.7	245	1.15	79.7	210	1.44	0.9989	81.6	207	1.80	0.9912
25	170	6	4.9	84.5	293	1.03	80.0	260	1.20	0.9998	82.1	283	1.32	0.9949
25	230	6	4.9	81.4	444	0.94	80.5	419	1.09	0.9980	82.3	416	1.39	09935
32	200	6	3.9	67.8	427	0.74	71.7	407	0.99	0.9809	72.5	450	1.05	0.9954
32	200	6	5.9	77.3	269	1.10	77.2	262	1.14	0.9861	78.1	298	1.19	0.9846
35	200	6	4.9	70.5	292	0.92	72.0	338	0.95	0.9899	73.7	361	1.07	0.9961

*adsorption capacities ($q_{cal,}$ q_{cal}) have been calculated to relative concentration of C/C_i = 0.95

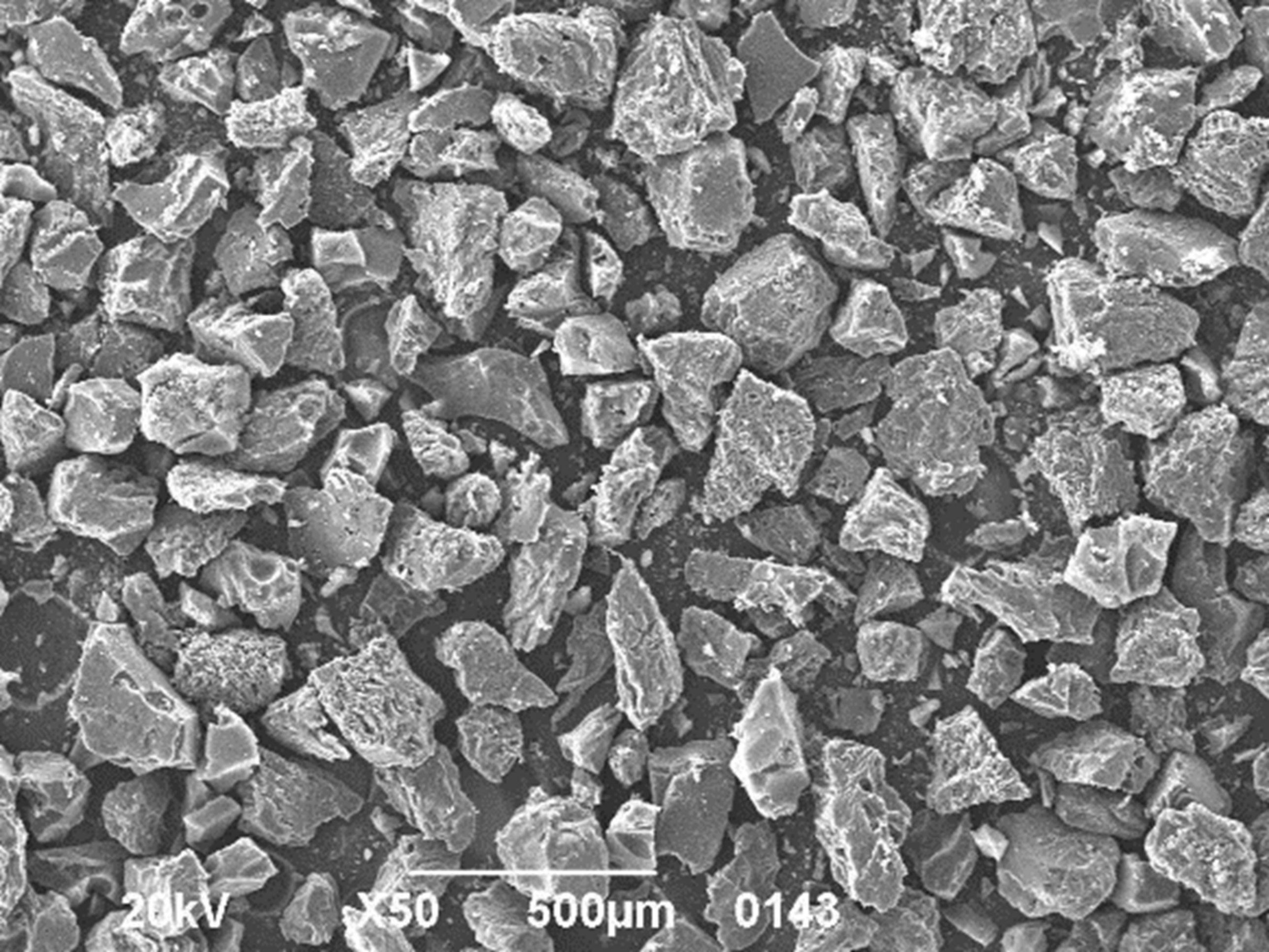
20kV X50 500µm 0143

Cooling circuit

Paracetamol solution circuit

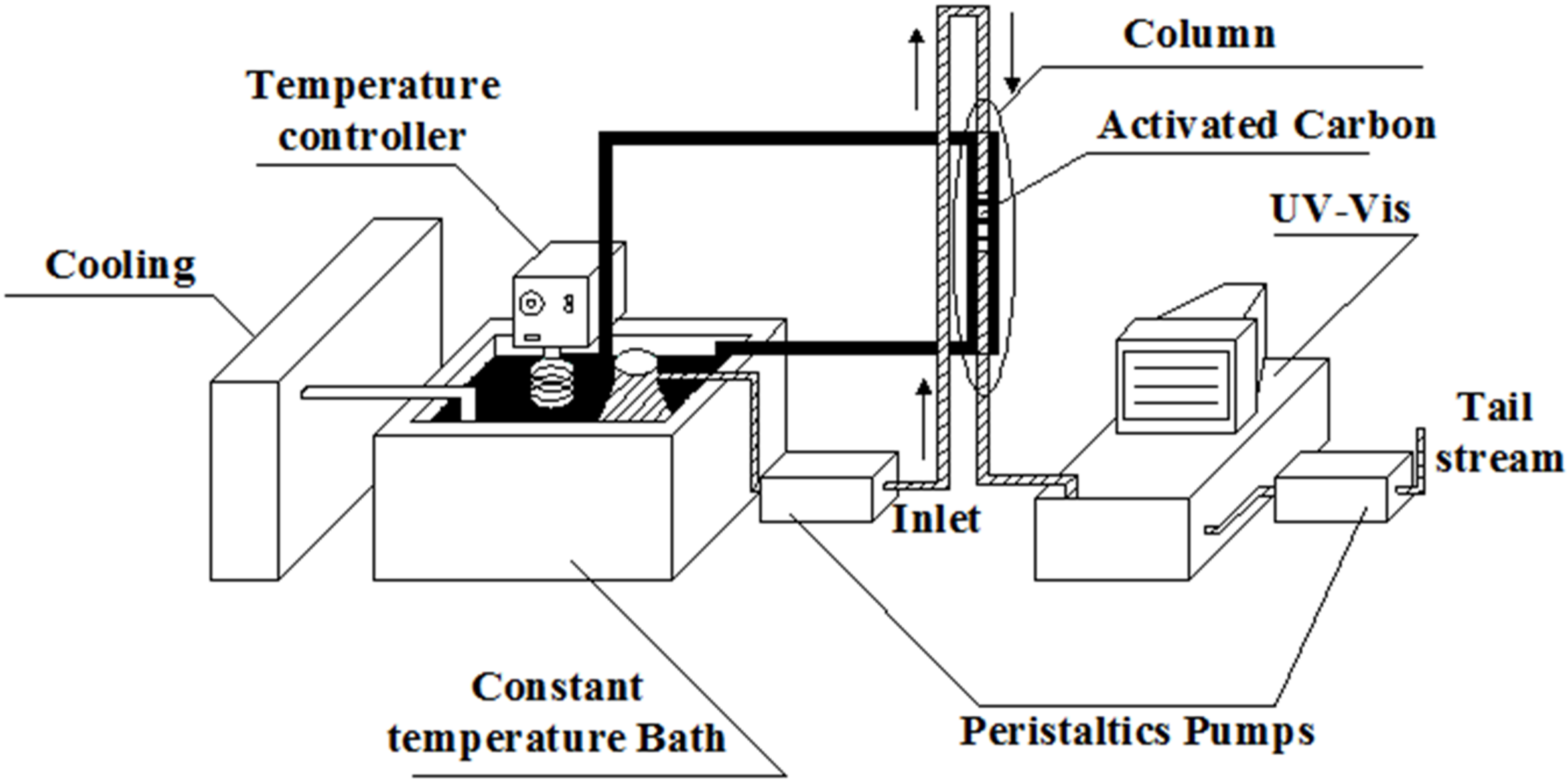

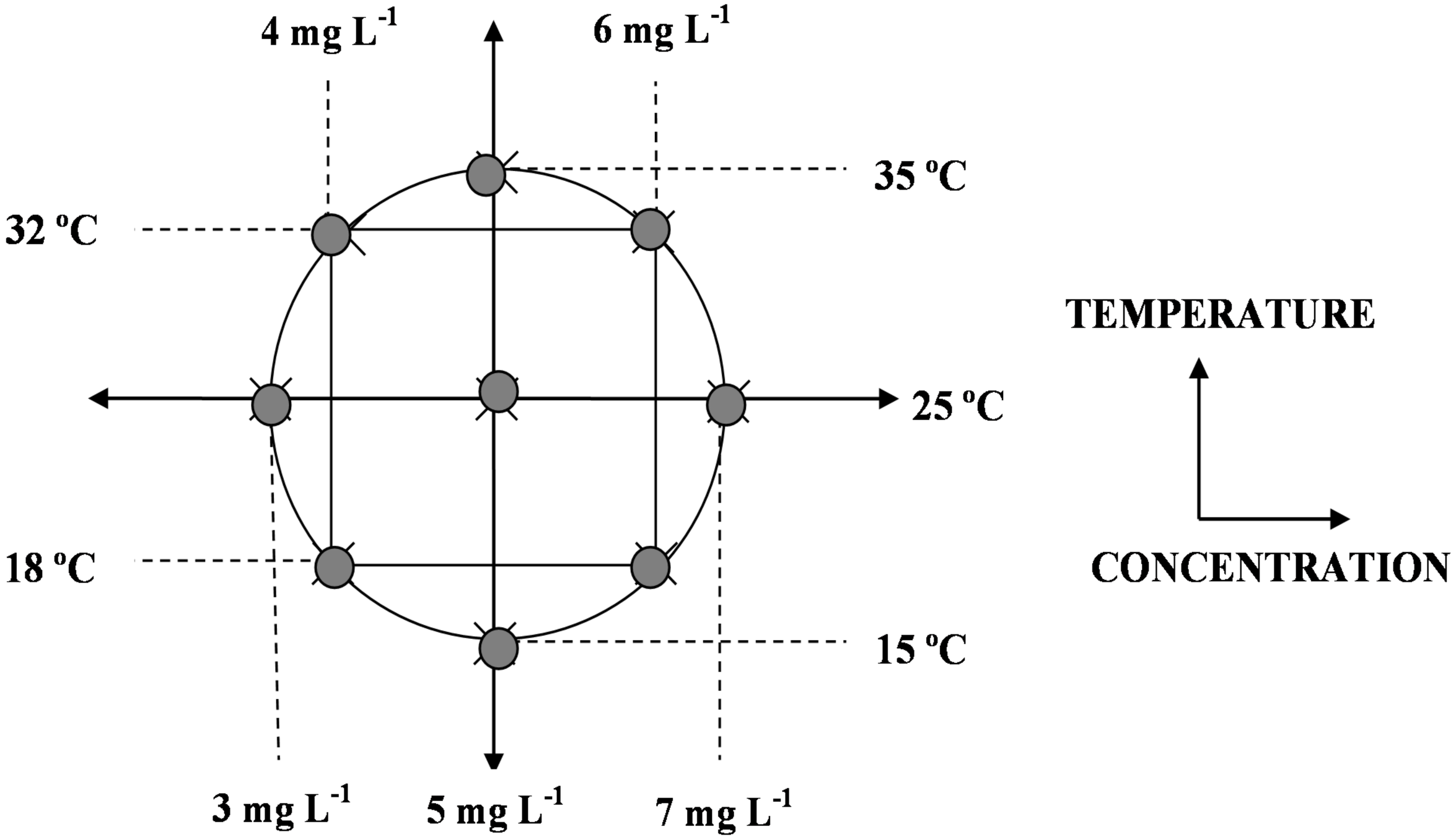
4 mg L-1
6 mg L-1
35 ºC
32 ºC
25 ºC
18 ºC
15 ºC
3 mg L-1
5 mg L-1
7 mg L-1
TEMPERATURE
CONCENTRATION

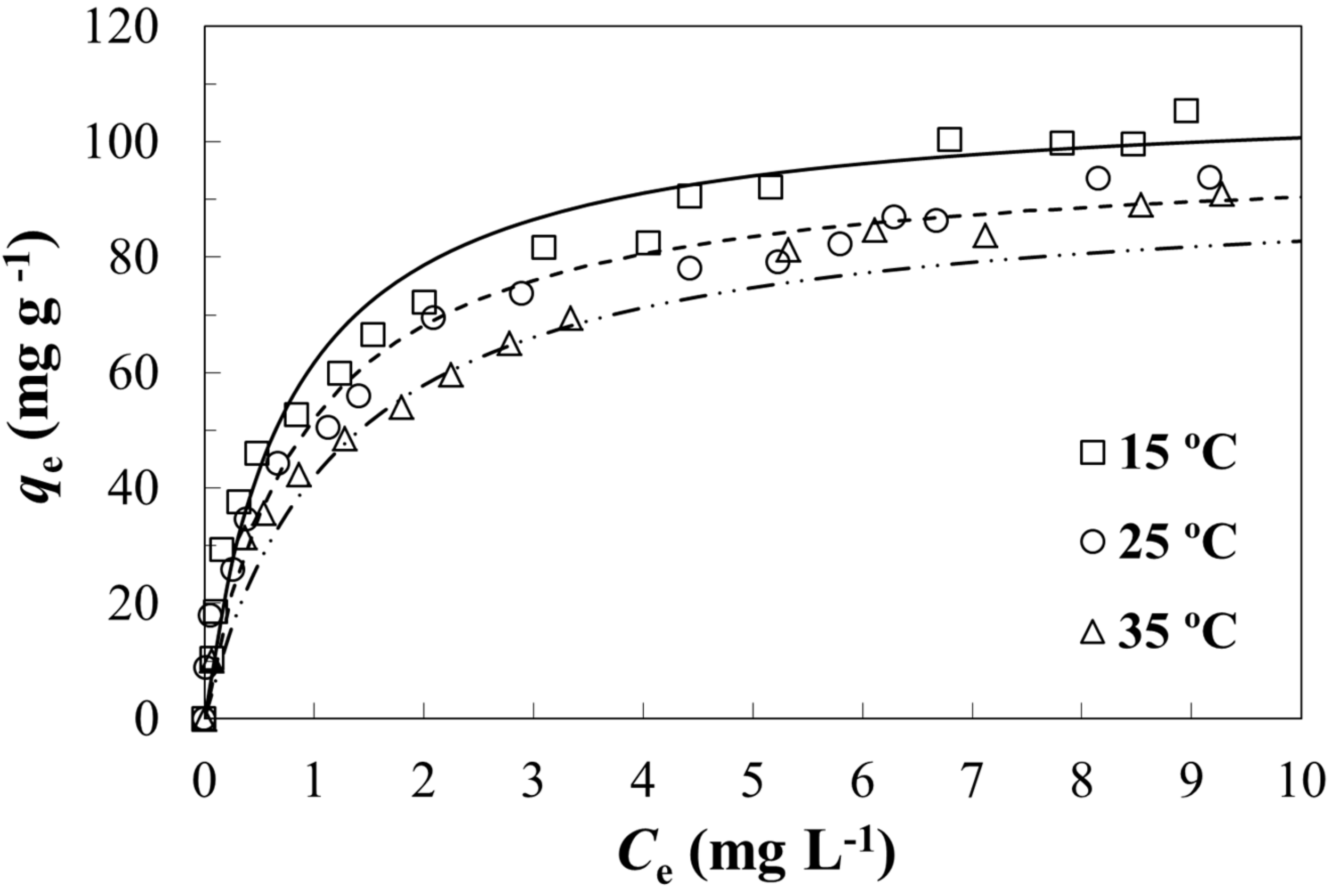
120
100
80
60
40
20
0
q_e (mg g-1)
0
1
2
3
4
5
6
7
8
9
10
C_e (mg L^{-1})
15 °C
25 °C
35 °C

a)

15 ºC
25 ºC
35 ºC

q_t (mg g^{-1})

50
40
30
20
10
0

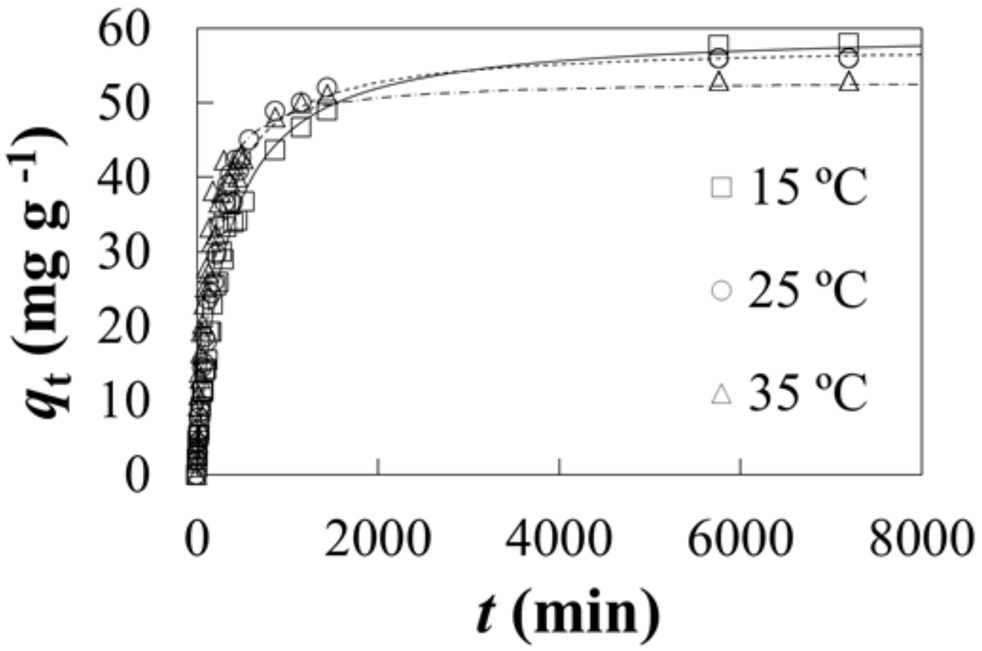

b)

—15 ºC
- - 25 ºC
—· 35 ºC

dq_t/dt (mg g^{-1}min^{-1})

0.6
0.5
0.4
0.3
0.2
0.1
0

0
100
200
300
400
500
600

t (min)

$B = 0.0028\ s^{-1}$ $r^2 = 0.976$

$B = 0.0017\ s^{-1}$ $r^2 = 0.991$

$B = 0.0011\ s^{-1}$ $r^2 = 0.992$

$\left(\sqrt{\pi} - \sqrt{\pi - \left(\pi^2 \cdot F(t)/3\right)}\right)^2$

2
1.8
1.6
1.4
1.2
1
0.8
0.6
0.4
0.2
0

0
250
500
750
1000
1250
1500

t (min)

● 15 ºC

■ 25 ºC

▲ 35 ºC

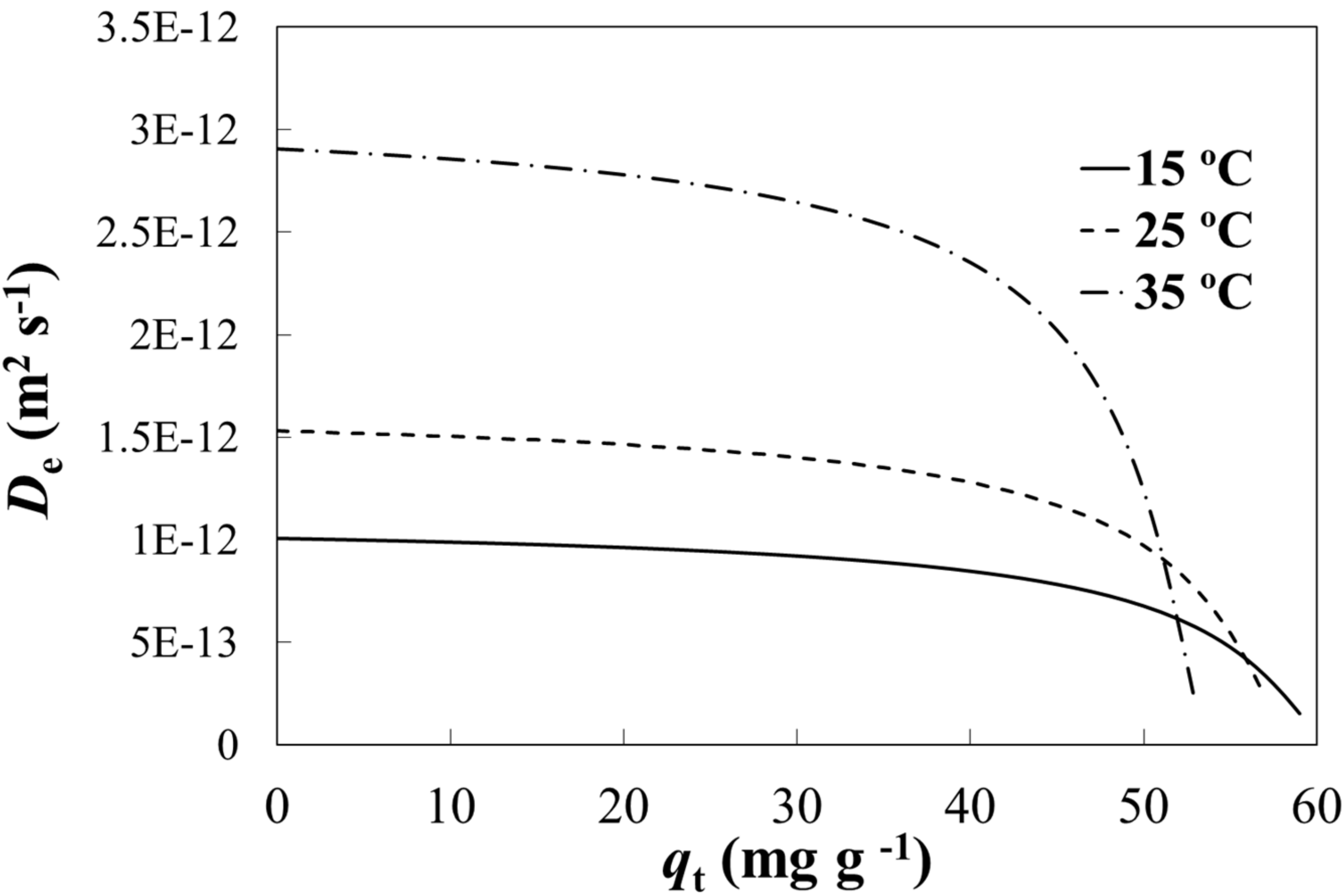
3.5E-12
3E-12
2.5E-12
2E-12
1.5E-12
1E-12
5E-13
0
D_e (m^2 s^{-1})
15 °C
25 °C
35 °C
0
10
20
30
40
50
60
q_t (mg g^{-1})

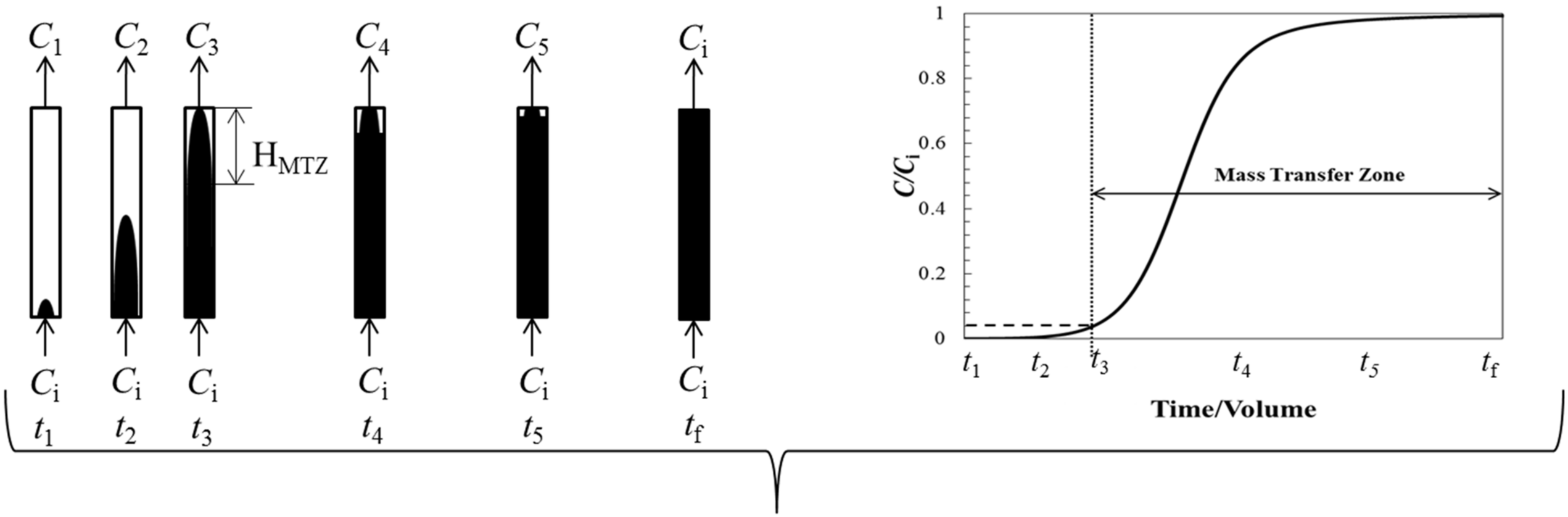
C_1
C_2
C_3
C_4
C_5
C_i
H_{MTZ}
C_i
t_1
t_2
t_3
t_4
t_5
t_f
1
0.8
0.6
0.4
0.2
0
C/C_i
Mass Transfer Zone
Time/Volume
Breakthrough profile
Adsorbent:
R_p, ε_p, ρ_b
Batch:
D_e, q_L, K_L
Empirical estimation:
D_z, k_f
75
74
73
i+1
i
i-1
6
5
4
3
2
1
Cb_{i+1}
$Cp_{i+1}= f(Cb_{i+1}, Cp_{i+1})$
q_{i+1}
Cb_i
$Cp_i= f(Cb_i, Cp_i)$
q_i
Cb_{i-1}
$Cp_{i-1}= f(Cb_{i-1}, Cp_{i-1})$
q_{i-1}
Convective flow
Diffusive flow
Adsorption rate
Experimental design
C_i, v_z, T, L_b

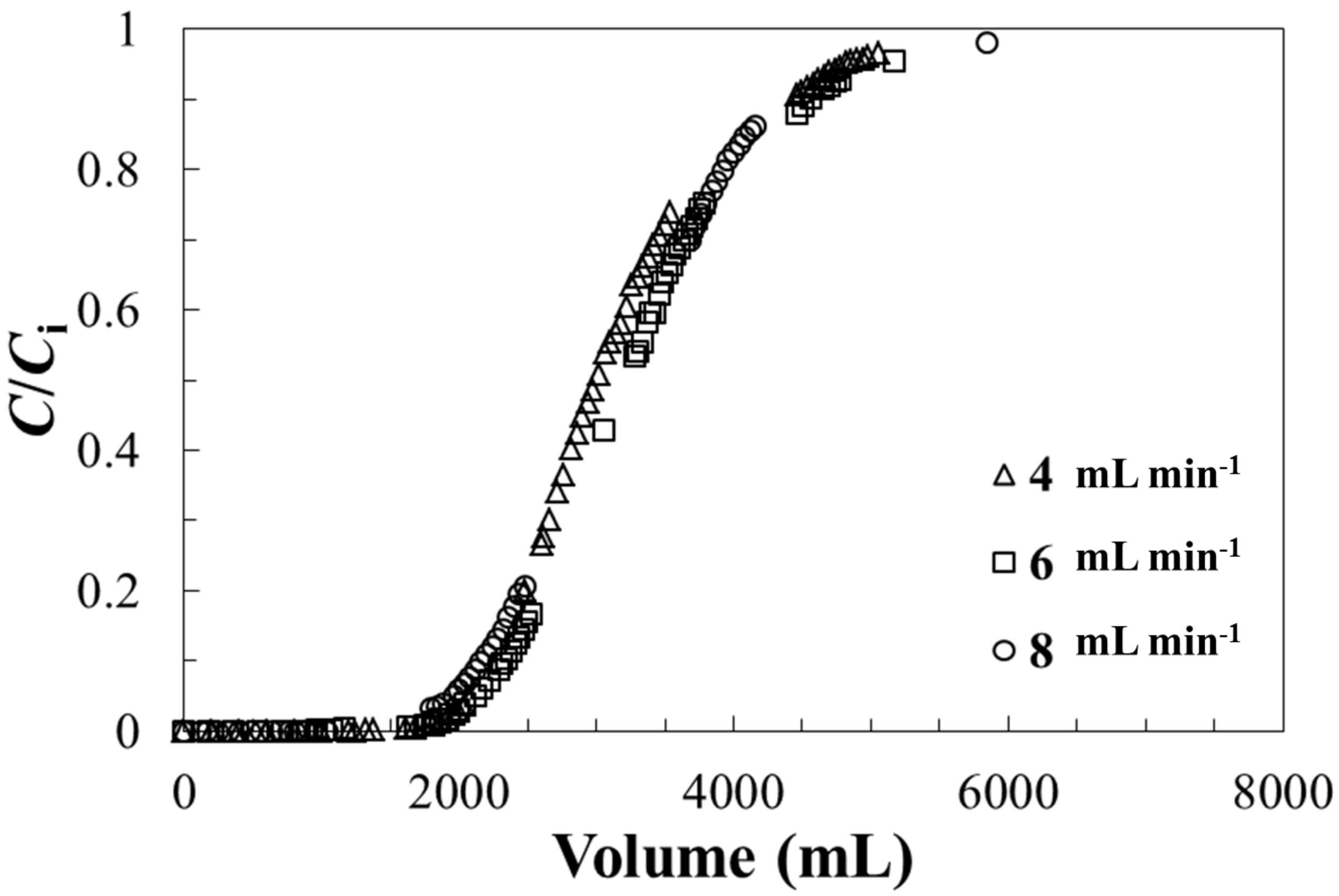
1
0.8
0.6
0.4
0.2
0
C/Ci
0
2000
4000
6000
8000
Volume (mL)
4 mL min-1
6 mL min-1
8 mL min-1

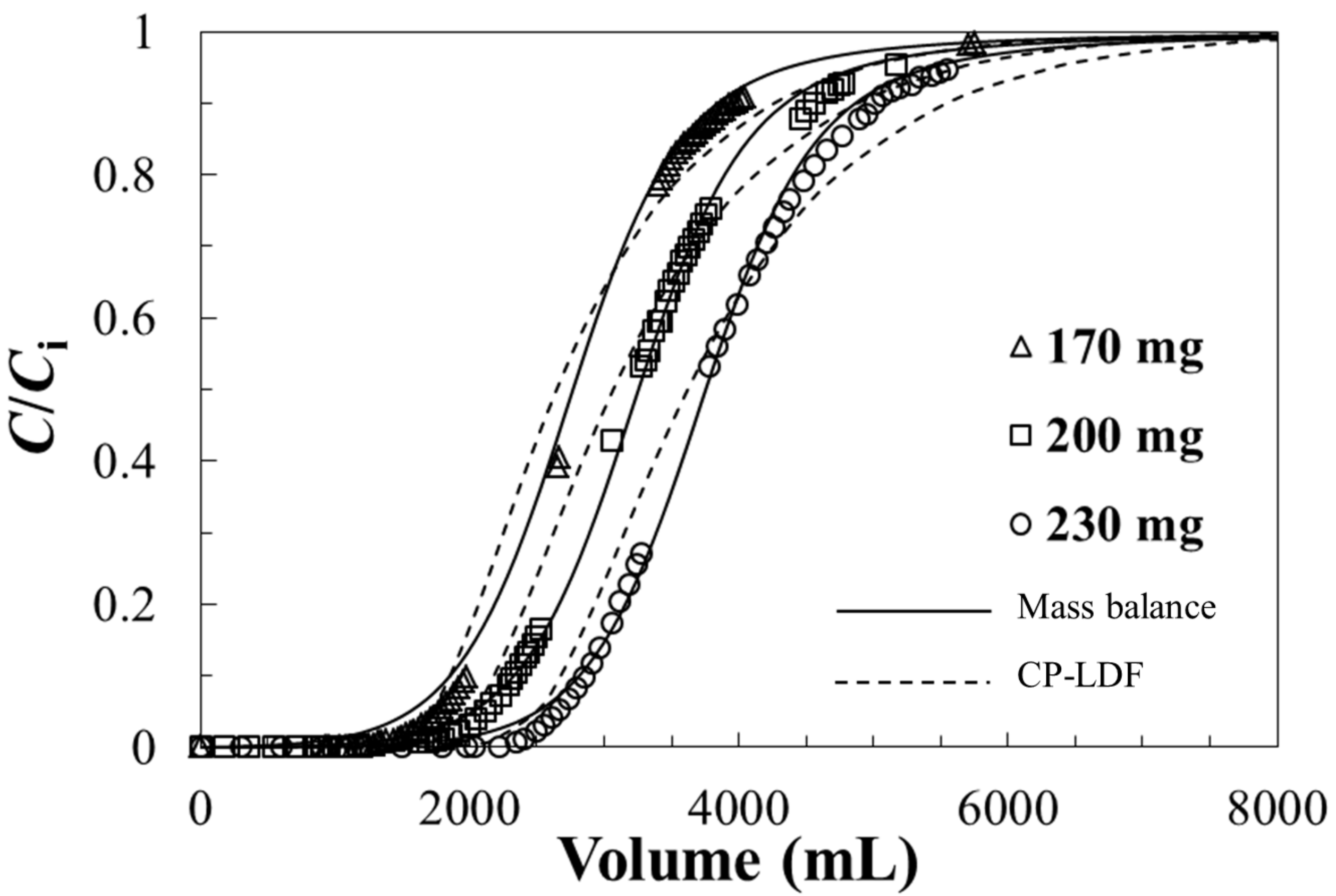
1
0.8
0.6
0.4
0.2
0
C/Ci
0
2000
4000
6000
8000
Volume (mL)
170 mg
200 mg
230 mg
Mass balance
CP-LDF

a)

C/C_i

1
0.8
0.6
0.4
0.2
0

15 °C
25 °C
35 °C
Mass balance
CP-LDF

b)

C/C_i

1
0.8
0.6
0.4
0.2
0

3 mg L^{-1}
5 mg L^{-1}
7 mg L^{-1}
Mass balance
CP-LDF

0
2000
4000
6000
8000

Volume (mL)

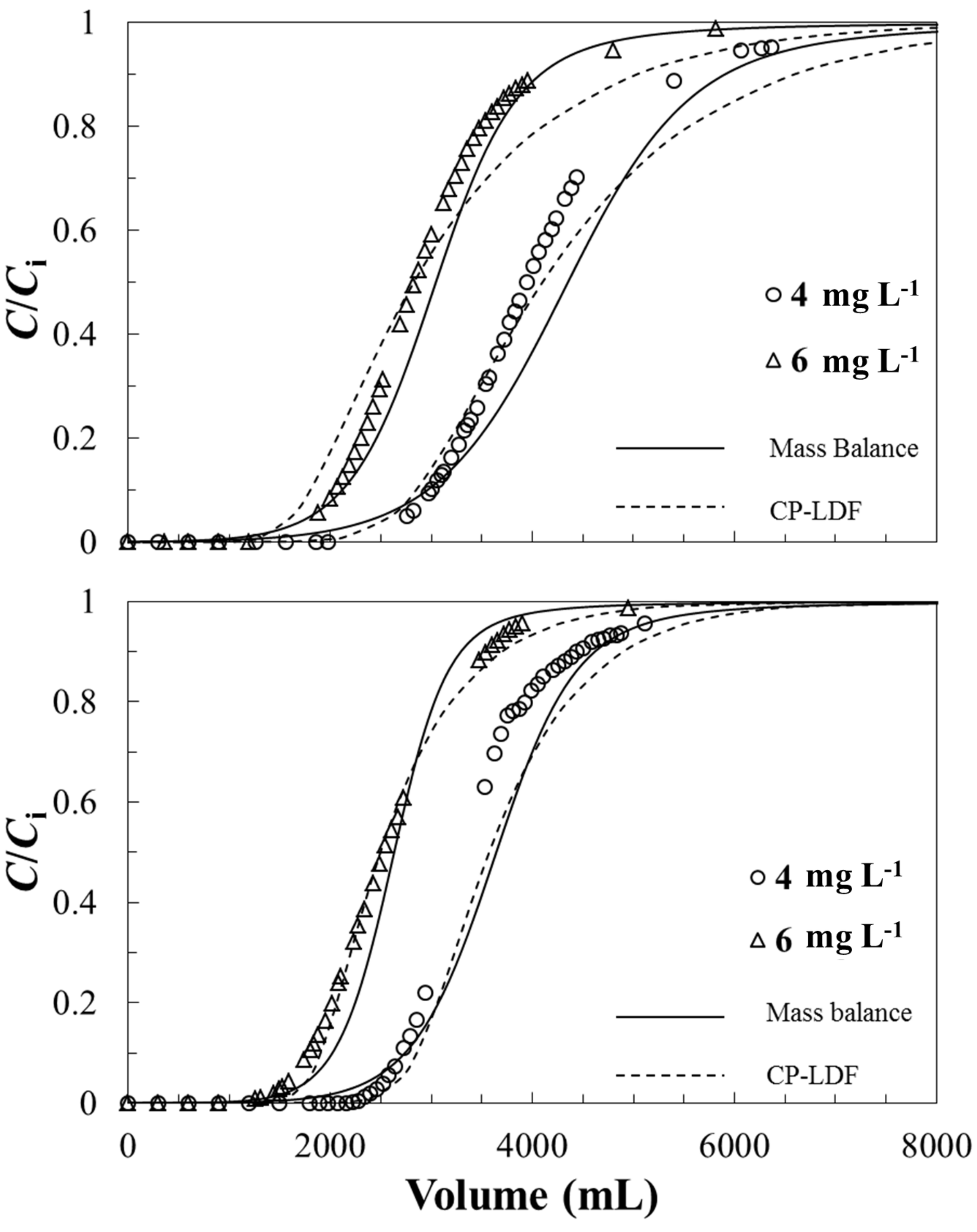
C/Ci
1
0.8
0.6
0.4
0.2
0
4 mg L-1
6 mg L-1
Mass Balance
CP-LDF
C/Ci
1
0.8
0.6
0.4
0.2
0
4 mg L-1
6 mg L-1
Mass balance
CP-LDF
0
2000
4000
6000
8000
Volume (mL)